Dopaminergic Co-transmission with Sonic Hedgehog Inhibits Expression of Abnormal Involuntary Movements

Authors: Lauren Malave[1,2], Dustin R. Zuelke[1,3], Lev Starikov[1,3], Heike Rebholz[1,8], Eitan Friedman[1], Chuan Qin[4], Qin Li[4,5], Erwan Bezard[4,5,6,7], and Andreas H. Kottmann[1,2,3,9].

[1] Department of Molecular, Cellular and Biomedical Sciences, CUNY School of Medicine at City College of New York, City University of New York, New York, NY, 10031, USA.
[2] City University of New York Graduate Center, Neuroscience Collaborative, New York City, NY 10031, USA
[3] City University of New York Graduate Center, Molecular, Cellular and Developmental Subprogram, New York City, NY 10031, USA
[4] Institute of Laboratory Animal Sciences, China Academy of Medical Sciences, Beijing City, People's Republic of China
[5] Motac Neuroscience, Manchester, UK
[6] Universite de Bordeaux, Institut des Maladies Neurodégénératives, UMR 5293, F-33000 Bordeaux, France
[7] CNRS, Institut des Maladies Neurodégénératives, UMR 5293, F-33000 Bordeaux, France
[8] present address: Danube Private University (DPU), Krems, Austria

[9]Corresponding author: (Andreas H. Kottmann, akottmann@med.cuny.edu)

Abstract/Summary:

Our limited understanding of neuronal co-transmission complicates predicting the effects of pharmacological interventions from neuronal wiring diagrams [1, 2]. For example, dopamine neurons (DAN), whose degeneration causes the motor and cognitive deficits of Parkinson's Disease (PD) [3], communicate with all their targets by dopamine (DA) and in addition use the neurotransmitters GABA, Glutamate and secreted peptides including the morphogen Sonic Hedgehog (Shh) to signal to select subsets of neurons [4-8]. It is unknown whether Levodopa (L-Dopa) induced dyskinesia (LID), a debilitating side effect of DA supplementation therapy in PD [9], might appear because DAN targets become exposed to high levels of DA but diminished levels of other DAN produced signaling factors. Here we show that restoring the balance of DA and Shh signaling by agonists of the Shh signaling effector G-protein coupled receptor Smoothened (Smo [10, 11]) attenuates LID in mouse- and macaque- models of PD. Using conditional genetic loss of function approaches of pre- and post-synaptic Shh signaling we found that reducing the activity of Smo selectively in cholinergic neurons facilitates LID. Conversely, the expression of a constitutive active form of Smo (SmoM2 [12]) in cholinergic neurons is sufficient to render the sensitized aphakia model of PD resistant to LID. Furthermore, the acute diminishment of Shh emanating from DAN by optogenetic means in the otherwise intact brain and in the absence of L-Dopa results in LID-like abnormal involuntary movements. We reveal that Shh co-transmission counteracts DA action in a DAN target- and striatal domain- specific manner. Our results suggest an un-anticipated mechanism - reduced Shh signaling - by which DAN degeneration sensitizes PD patients to LID. We anticipate that our models provide a starting point for assessing the contributions of Shh to the "teaching" signal that emanates from DAN and testing the hypothesis that LID are caused by aberrant learning [13-15].

Main:

Previous work has implicated aberrant cholinergic activity in LID in PD models but mechanistic details remain ill-defined since both boosting as well as inhibiting cholinergic signaling were found to attenuate LID [16-22]. These divergent results are likely a reflection of the post synaptic complexity of cholinergic signaling in the striatum [23]. Hence, normalizing cholinergic activity at the level of CIN themselves might prevent the formation of LID and preserve the contribution of regulated CIN activity to striatal function. In the healthy brain, DAN engage CIN as a relay hub to control striatal circuits by patterning cholinergic activity [24, 25]: DA inhibits CIN through binding to D2 receptor (D2R) resulting in the pause of the "burst-pause-burst" firing pattern of CIN in response to reward-related cues or outcomes [26, 27] [28, 29]. Unfortunately, how DAN degeneration results in aberrant CIN activity is also not well understood [30]. For example, as DA

levels fall in the PD brain, cholinergic signaling strength rises [31], yet acetylcholine availability becomes reduced concomitantly with progressive DAN deficiency in murine models [32] suggesting that relative rather than absolute levels of cholinergic tone might change in PD. Recently it was found that dopaminergic co-transmission with glutamate supports the rebound of firing of CIN located in the dorso-lateral striatum (DLS) after a DA induced pause in firing [7]. Since CIN express the Shh receptor Patched (Ptc1) [8], we investigated whether reduced levels of Shh expressed by DAN (Shh_{DAN}) might play a role in LID.

DAN degeneration must cause a diminishment of DA as well as Shh_{DAN}. Therefore, L-Dopa treatment without augmenting Shh signaling must result in a drug-induced imbalance of high DA and low Shh signaling onto CIN compared to the situation in the healthy brain (Fig. 1 A). Hence, we tested first whether augmenting Shh signaling during L-Dopa therapy would attenuate dyskinesia in preclinical models of LID. LID is quantified by a subjective measure called the abnormal involuntary movement (AIM) scale [33]. Related behavioral tests with predictive validity have been developed in rodent and non-human primate models based on genetic- or neurotoxin- induced degeneration of DAN [9, 34]. In the 6-OHDA model, the unilateral striatal injections of the dopaminergic toxin 6-OHDA results in dopaminergic denervation of the ipsilateral striatum and rotational bias (extended data Fig. 1). Daily injections of L-Dopa (5 mg/kg L-Dopa) results in the appearance of unilateral AIMs (Fig. 1 B). Repeated co-injection of L-Dopa with the Smo antagonist cyclopamine [35] (Cyclo, 5 mg/kg) increases AIM scores (Fig 1 B, red bars), while, conversely, repeated co-injection of the Smo agonist SAG [11] (0.8, 2.5 or 7 mg/kg) results in dose dependent attenuation of AIMs (Fig. 1 B, blue bars). The SAG effect on LID is rapidly reversible and can be elicited repeatedly in the same cohort of animals (extended data, Fig. 2).

In the aphakia (*AK*$^{-/-}$) mouse line the absence of the transcription factor Pitx3 results in the bilateral, partial loss of dopaminergic innervation of the dorsal striatum [36, 37]. Daily injection of *AK*$^{-/-}$ mice with L-Dopa (25 mg/kg) resulted in LID [38] (Fig. 1 C). Repeated co-injections of L-Dopa with Cyclo (5 mg/kg) resulted in increased AIMs (Fig. 1 C, red bar) while, in contrast, daily co-injections of L-Dopa with SAG (20 mg/kg) resulted in a threefold attenuation of AIM (Fig. 1 C, blue bar).

Remarkably, co-injection of a single dose of the Smo agonists Purmorphamine [39] (PUR, 15 mg/kg) or SAG (10 mg/kg) with the last daily dose of L-Dopa reduced AIMs in the 6-OHDA model (Fig. 1 D). Similarly, in the *AK*$^{-/-}$ mice a single dose of SAG (20 mg/kg) co-administered with L-Dopa at the last day of L-Dopa dosing reduced AIMs to the same degree achieved with the clinical effective anti-dyskinetic drug amantadine (AM, 60 mg/kg) [40], while the combination of SAG (20 mg/kg) and AM (60 mg/kg) resulted in the additive attenuation of AIMs (Fig. 1 E). A dose response study revealed that the dose of SAG needed to attenuate LID is positively and linearly correlated with the L-Dopa dose used to induce LID (extended data Fig. 3). These experiments indicated that the acute, relative imbalance of Smo- and DA- signaling determines the severity LID.

In Parkinsonian Macaques repeated dosing with L-Dopa results in LID that can be blunted by AM [41]. Co-injection of SAG (3, 9, and 27 mg/kg) together with L-Dopa attenuated LID at the highest dose during the first 2 hours of a 200 min long bout of LID (Fig. 1 F; extended data Fig. 4 A). In contrast to AM, and of translational significance, neither the chronic nor the acute dosing with SAG reduced the anti-akinetic benefit of L-Dopa in any of the three animal models tested (extended data Fig. 4 B-D).

Early during the establishment of LID, pErk$^{1/2}$ (phospho-Thr202/Tyr204–ERK1/2) is

found in a dispersed pattern in the striatum and involves mainly medium spiny projection neurons. However, in response to chronic dosing with L-Dopa pErk$^{1/2}$ prevalence increases progressively among CINs in the DLS in correlation with LID severity [19]. Consistent with the aforementioned behavioral responses, daily L-Dopa injections paired with either inhibition (Cyclo) or stimulation (SAG) of Smo resulted in an increase (red bars) or decrease (blue bars), resp., of the fraction of pErk$^{1/2}$ positive CINs in the DLS but not in the dorsomedial striatum (DMS) in 6-OHDA lesioned - and AK$^{-/-}$ - mice 30 min after the final L-Dopa injection (Fig. 1 G, H). Similarly, a single dose of the Smo agonists SAG or PUR paired with the last daily dose of L-Dopa reduced the prevalence of pErk$^{1/2}$ positive CINs in the DLS but not DMS in both paradigms (Fig. 1 I). Together, the data derived from distinct models revealed that Smo activity modulates LID in a reversible, bi-directional, immediate and dose dependent manner that correlates with MAP kinase pathway activity in CINs of the DLS.

FIGURE 1

If Smo expressed by CINs is the relevant target of the Smo antagonist and agonist treatment that either facilitates or attenuates, resp., LID in the aforementioned paradigms then the conditional loss or gain of function of Smo in cholinergic neurons should result in the facilitation or attenuation, resp., of LID as well. Consistent, in mice with selective ablation of Smo from cholinergic neurons ($Smo_{ChAT\text{-}Cre}^{-/-}$, Fig. 2 A; all recombinant mouse strains and their controls used in this study are referenced in Methods) daily L-Dopa dosing (25 mg/kg, Fig. 2 B) resulted in a Smo gene dosage dependent appearance of LID (Fig. 2 C) and a corresponding increase in the fraction of pErk$^{1/2}$ positive CIN in the DLS (extended data Fig. 5 A). Conversely, in $AK^{-/-}$ mice that express the constitutive active form of Smo, the oncogene SmoM2 [12], selectively in cholinergic neurons ($SmoM2_{ChAT\text{-}Cre}^{+/-}; AK^{-/-}$, Fig. 2 D, extended data Fig. 6) daily L-Dopa dosing

(25 mg/kg, Fig. 2 E) resulted in a blockade of LID that developed in controls (Fig. 2 F) and a corresponding decrease in the prevalence of pErk$^{1/2}$ positive CIN in the DLS (extended data Fig. 5 B).

Smo is tonically inhibited by the resistance-nodulation-cell division (RND) like transmembrane transporter protein Ptc1 [42], which is the receptor for Shh [43] and is expressed by CINs [8]. Shh binding to Ptc1 relieves the inhibition of Smo [42]. The conditional expression of myristylated GFP (myrGFP) in Shh expressing cells (Methods) reveals the greatest density of Shh carrying neuropil in the DLS (extended data Fig. 7) suggesting greater Shh signaling strength in the DLS compared to the DMS. One potentially relevant source of Shh for the regulation of Smo activity in CIN in the DLS are DAN of the Substantia Nigra pars compacta (SNpc), which express Shh throughout life [8], target CIN of the DLS [44] and degenerate in PD [32]. We found that mice with selective ablation of Shh from DAN ($Shh_{DAN}^{-/-}$ [8] Fig. 2 G) displayed dose dependent AIMs in response to daily dosing with L-Dopa (10 mg/kg or 25 mg/kg; Fig. 2 H, I). LID established by daily injections of 25 mg/kg L-Dopa for 20 days in $Shh_{DAN}^{-/-}$ mice (Fig. 2 K) can be attenuated dose-dependently by a single dose of SAG (10 or 20 mg/kg) co-administered with the final dose of L-Dopa (Fig. 2 L). Further, L-Dopa dosing in $Shh_{DAN}^{-/-}$ mice resulted in an increase in the fraction of pErk^{1,2} positive CIN in the DLS, which could be normalized by SAG (Fig. 2 M, N), but had no effect on pErk^{1,2} prevalence in the DMS (Fig. 2 N). Thus, these genetic manipulations establish that Shh_{DAN} is a relevant agent for Smo modulation in CIN in the DLS and reveal that pre- or post-synaptic interruption of Shh/Smo signaling between DAN and CIN facilitates LID while, conversely, constitutive Smo activation in CIN blocks LID expression in the sensitized $AK^{-/-}$ model.

FIGURE 2

We next investigated whether AIMs could be observed by producing an acute diminishment of Shh_{DAN} signaling in the intact brain and without L-Dopa dosing. In general, neuropeptide release is triggered by prolonged high frequency stimulation [2, 45] and, concordant, burst stimulation of hippocampal neurons elicits Shh release [46]. This observation suggested the possibility that optogenetically forced, prolonged burst stimulation of DAN might provide an experimental approach for the exhaustion of releasable Shh from DAN over time. Consistent, we found that unilateral pulsatile burst firing of DAN (Fig. 3 A, Methods; stimulation regiment as in ref. [46]) results in stimulation-dependent rotational activity that intensifies over the course of an hour (Fig. 3 B) without changing dopaminergic fiber density (extended data Fig. 8). The injection of Cyclo (5 mg/kg) 30 min prior to onset of optogenetic stimulation elicited a maximal rotational response immediately at the beginning of stimulation rather than only after one hour as seen in controls (Fig. 3 C). Conversely, injection of SAG 30 min prior to onset of optogenetic stimulation blocked the gradual increase in circling behavior seen in controls (Fig. 3 D). These results suggested that optogenetic stimulation of DAN might result in gradual reduced Shh_{DAN} signaling in CIN over the course of an hour leading to a situation, which, in the $Shh_{DAN}^{-/-}$, $Smo_{ChAT\text{-}Cre}^{-/-}$, $AK^{-/-}$ mice and in 6-OHDA lesioned animals, facilitates LID.

Concordant, we find LID-like axial and limb AIMs time-locked with stimulation in the last 10 minutes, but not in the first 10 minutes of the first hour of optogenetic stimulation (Fig. 3 E; extended data video OID day 1 control; Methods). Daily repeated one hour stimulation sessions resulted in an intensification of AIMs, which we termed optogenetic induced dyskinesia (OID): on day 10 orofacial (tongue protrusions) movements in addition to abnormal axial and limb movements were observed and OID behavior appeared already during the first 10 minutes of stimulation which then further increased in intensity during the remainder of the session (Fig. 3

E, extended data video OID day 9). A single dose of SAG (20 mg/kg) administered prior to optogenetic stimulation attenuated axial, limb and orofacial OID (Fig. 3 E). These results indicate that optogenetic stimulation of DAN in the otherwise intact brain and without L-Dopa results in LID-like AIMs within minutes of onset of pulsatile burst stimulation that escalate in magnitude by repeated daily stimulation sessions and are caused in part by reduced Smo activation.

FIGURE 3

We next examined whether Shh_{DAN}/Smo signaling effects the levels of the neuronal activity marker p-rpS6$^{240/244}$ in CIN which were shown previously to correlate positively with CIN activity under basal and stimulated conditions [47-49].

Concordant with the previous finding that cholinergic tone in the striatum, as measured by in vivo dialysis, was reduced 8-fold in $Shh_{DAN}^{-/-}$ mice [8], we found reduced p-rpS6$^{240/244}$ levels in $Shh_{DAN}^{-/-}$ mice compared to controls (Fig 4 A, B; extended data Fig. 9). A single dose of SAG (20 mg/kg) alone or together with L-Dopa (25mg/kg) 30 min prior to analysis normalized p-rpS6$^{240/244}$ levels in $Shh_{DAN}^{-/-}$ mice (Fig. 4 A, B) indicating that Smo activity boosts CIN activity even in the presence of L-Dopa. The selective ablation of Smo from cholinergic neurons in $Smo_{ChAT\text{-}Cre}^{-/--}$ animals phenocopied the reduction in p-rpS6$^{240/244}$ levels in CIN found in $Shh_{DAN}^{-/-}$ mice (Fig. 4 C, D). However, SAG failed to normalize diminished levels of p-rpS6$^{240/244}$ in CIN of $Smo_{ChAT\text{-}Cre}^{-/-}$ animals demonstrating that Shh_{DAN} boosts p-rpS6$^{240/244}$ levels through Smo activation in CIN (Fig. 4 C, D). Average p-rpS6$^{240/244}$ levels in CIN of mice expressing the constitutive active SmoM2 in CIN ($SmoM2_{ChAT\text{-}Cre}^{+/-}$mice) were not increased suggesting that basal levels of Shh signaling results in maximal p-rpS6$^{240/244}$ levels in CINs (Fig. 4 C, D). Further, one hour of optogenetic stimulation of DAN results in decreased p-rpS6$^{240/244}$ levels in

CIN of the stimulation ipsilateral DLS compared to the unstimulated contralateral control side (Fig. 4 E, F). Decreased p-rpS6$^{240/244}$ levels in CIN could be normalized by SAG administration prior to onset of optogenetic stimulation (Fig. 4 E, F). These observations indicate that long term as well as semi-acute reduction of Shh_{DAN}/Smo signaling by pre- or post- synaptic manipulations results in decreased CIN activity.

FIGURE 4

In summary we employed well established macaque and mouse models and developed novel genetic and optical stimulation paradigms for manipulating the relative strength of DA and Shh co-transmission by DAN onto CIN in the context of LID (Fig 4 G). Consistent across paradigms, we observe that LID like AIMs are caused by a diminishment of Shh_{DAN}/Smo signaling onto CIN of the DLS, and conversely, that boosting Smo signaling in CIN long-term or within minutes attenuates AIMs through a mechanism that resides upstream of the cholinergic modulation of striatal output pathways (Fig 4 G; extended data Fig. 10). These findings reveal an unanticipated mechanism, reduced levels of Shh_{DAN}, by which degeneration of DAN in PD predisposes to LID and indicate interesting directions for further study and clinical translation. For example, our data provides a strong rationale for exploiting effectors of Smo signaling in CIN for the development of anti-LID medication. Further, our findings suggest that Shh_{DAN} must be considered to be part of the physical identity of the “teaching” signal that emanates from DAN and it will be of interest to determine the role of Shh_{DAN} in reinforcement learning. Furthermore, our results provide a strong rationale to investigate whether cognitive deficits in PD [50] and behavioral addictions that emerge in L-Dopa treated PD patients [51] can be attenuated by manipulating the balance of Shh/Smo- and dopamine- signaling.

Acknowledgements:

This work was supported by the American Parkinson Disease Association, Research Foundation of the City University of New York, and NIH NS095253 to A.H.K., and in part by NIH R25GM56833 (P.I. Mark Steinberg) via a "RISE" fellowship to L.M. L.M., D.R.Z, and L.S. acknowledge administrative-, travel- and mentoring- support they received through the graduate programs in biology of the Graduate Center of the City University of New York. A.H.K. thanks John Martin for active mentoring and support throughout. L.M. and A.H.K. thank Luis Gonzalez-Reyes for help with statistical analyses. We are grateful to Y.J.Z., L.H., C.Y.L., and X.R.L for the care of the non-human primates. We thank, Paul Forlano, Christoph Kellendonk, John Martin, Stephen Rayport and Santiago Uribe-Cano for their critical comments on earlier versions of the manuscript.

Contributions:

L.M., D.R.Z. and A.H.K designed all mouse experiments. A.H.K. wrote the paper. L.M. and D.R.Z. carried out all mouse experiments and surgeries with contributions from L.S.. L.M., D.R.Z. and H.R. analyzed data. H.R. and E.F. contributed to neurotoxic LID paradigm analysis. D.R.Z. developed the optogenetic Shh exhaustion paradigm. C.Q., L.Q. and E.B. conducted the NHP experiments and analyzed the related data. E.B. contributed to writing the manuscript. A.H.K. supervised all aspects of the work.

Corresponding author

Correspondence to Andreas H. Kottmann, akottmann@med.cuny.edu.

Ethics declarations

The authors declare no competing interests.

Data availability:

All data that support the finding of this study are available upon request from the corresponding author.

References:

1. Granger, A.J., M.L. Wallace, and B.L. Sabatini, *Multi-transmitter neurons in the mammalian central nervous system.* Curr Opin Neurobiol, 2017. **45**: p. 85-91.
2. Nusbaum, M.P., D.M. Blitz, and E. Marder, *Functional consequences of neuropeptide and small-molecule co-transmission.* Nat Rev Neurosci, 2017. **18**(7): p. 389-403.
3. Schneider, S.A. and J.A. Obeso, *Clinical and pathological features of Parkinson's disease.* Curr Top Behav Neurosci, 2015. **22**: p. 205-20.
4. Rayport, S., et al., *Identified postnatal mesolimbic dopamine neurons in culture: morphology and electrophysiology.* The Journal of neuroscience : the official journal of the Society for Neuroscience, 1992. **12**(11): p. 4264-80.
5. Trudeau, L.E., et al., *The multilingual nature of dopamine neurons.* Progress in brain research, 2014. **211**: p. 141-64.
6. Chuhma, N., et al., *Heterogeneity in Dopamine Neuron Synaptic Actions Across the Striatum and Its Relevance for Schizophrenia.* Biological psychiatry, 2017. **81**(1): p. 43-51.
7. Chuhma, N., et al., *Dopamine neuron glutamate cotransmission evokes a delayed excitation in lateral dorsal striatal cholinergic interneurons.* Elife, 2018. **7**.
8. Gonzalez-Reyes, L.E., et al., *Sonic hedgehog maintains cellular and neurochemical homeostasis in the adult nigrostriatal circuit.* Neuron, 2012. **75**(2): p. 306-19.
9. Bastide, M.F., et al., *Pathophysiology of L-dopa-induced motor and non-motor complications in Parkinson's disease.* Progress in neurobiology, 2015. **132**: p. 96-168.
10. van den Heuvel, M. and P.W. Ingham, *smoothened encodes a receptor-like serpentine protein required for hedgehog signalling.* Nature, 1996. **382**(6591): p. 547-51.
11. Frank-Kamenetsky, M., et al., *Small-molecule modulators of Hedgehog signaling: identification and characterization of Smoothened agonists and antagonists.* Journal of biology, 2002. **1**(2): p. 10.
12. Riobo, N.A., et al., *Activation of heterotrimeric G proteins by Smoothened.* Proc Natl Acad Sci U S A, 2006. **103**(33): p. 12607-12.
13. Beeler, J.A., et al., *Dopamine-dependent motor learning: insight into levodopa's long-duration response.* Annals of neurology, 2010. **67**(5): p. 639-47.
14. Beeler, J.A., et al., *A role for dopamine-mediated learning in the pathophysiology and treatment of Parkinson's disease.* Cell Rep, 2012. **2**(6): p. 1747-61.
15. Zhuang, X., P. Mazzoni, and U.J. Kang, *The role of neuroplasticity in dopaminergic therapy for Parkinson disease.* Nature reviews. Neurology, 2013. **9**(5): p. 248-56.
16. Shen, W., et al., *M4 Muscarinic Receptor Signaling Ameliorates Striatal Plasticity Deficits in Models of L-DOPA-Induced Dyskinesia.* Neuron, 2016. **90**(5): p. 1139.
17. Bordia, T., et al., *Optogenetic activation of striatal cholinergic interneurons regulates L-dopa-induced dyskinesias.* Neurobiology of disease, 2016. **91**: p. 47-58.

18. Won, L., et al., *Striatal cholinergic cell ablation attenuates L-DOPA induced dyskinesia in Parkinsonian mice.* The Journal of neuroscience : the official journal of the Society for Neuroscience, 2014. **34**(8): p. 3090-4.
19. Ding, Y., et al., *Enhanced striatal cholinergic neuronal activity mediates L-DOPA-induced dyskinesia in parkinsonian mice.* Proceedings of the National Academy of Sciences of the United States of America, 2011. **108**(2): p. 840-5.
20. Quik, M., et al., *Nicotine-mediated improvement in L-dopa-induced dyskinesias in MPTP-lesioned monkeys is dependent on dopamine nerve terminal function.* Neurobiology of disease, 2013. **50**: p. 30-41.
21. Quik, M., et al., *Nicotine reduces established levodopa-induced dyskinesias in a monkey model of Parkinson's disease.* Movement disorders : official journal of the Movement Disorder Society, 2013. **28**(10): p. 1398-406.
22. Zhang, D., et al., *Nicotinic receptor agonists reduce L-DOPA-induced dyskinesias in a monkey model of Parkinson's disease.* The Journal of pharmacology and experimental therapeutics, 2013. **347**(1): p. 225-34.
23. Conti, M.M., N. Chambers, and C. Bishop, *A new outlook on cholinergic interneurons in Parkinson's disease and L-DOPA-induced dyskinesia.* Neurosci Biobehav Rev, 2018. **92**: p. 67-82.
24. Kawaguchi, Y., et al., *Striatal interneurones: chemical, physiological and morphological characterization.* Trends Neurosci, 1995. **18**(12): p. 527-35.
25. Kreitzer, A.C., *Physiology and pharmacology of striatal neurons.* Annu Rev Neurosci, 2009. **32**: p. 127-47.
26. Morris, G., et al., *Coincident but distinct messages of midbrain dopamine and striatal tonically active neurons.* Neuron, 2004. **43**(1): p. 133-43.
27. Schulz, J.M. and J.N. Reynolds, *Pause and rebound: sensory control of cholinergic signaling in the striatum.* Trends in neurosciences, 2013. **36**(1): p. 41-50.
28. Zhang, Y.F. and S.J. Cragg, *Pauses in Striatal Cholinergic Interneurons: What is Revealed by Their Common Themes and Variations?* Front Syst Neurosci, 2017. **11**: p. 80.
29. Kharkwal, G., et al., *Parkinsonism Driven by Antipsychotics Originates from Dopaminergic Control of Striatal Cholinergic Interneurons.* Neuron, 2016. **91**(1): p. 67-78.
30. Borgkvist, A., O.J. Lieberman, and D. Sulzer, *Synaptic plasticity may underlie l-DOPA induced dyskinesia.* Curr Opin Neurobiol, 2018. **48**: p. 71-78.
31. Barbeau, A., *The pathogenesis of Parkinson's disease: a new hypothesis.* Can Med Assoc J, 1962. **87**: p. 802-7.
32. McKinley, J.W., et al., *Dopamine Deficiency Reduces Striatal Cholinergic Interneuron Function in Models of Parkinson's Disease.* Neuron, 2019. **103**(6): p. 1056-1072 e6.
33. Mera, T.O., M.A. Burack, and J.P. Giuffrida, *Objective motion sensor assessment highly correlated with scores of global levodopa-induced dyskinesia in Parkinson's disease.* J Parkinsons Dis, 2013. **3**(3): p. 399-407.
34. Sebastianutto, I., et al., *Validation of an improved scale for rating l-DOPA-induced dyskinesia in the mouse and effects of specific dopamine receptor antagonists.* Neurobiology of disease, 2016. **96**: p. 156-170.
35. Chen, J.K., et al., *Small molecule modulation of Smoothened activity.* Proceedings of the National Academy of Sciences of the United States of America, 2002. **99**(22): p. 14071-6.
36. Nunes, I., et al., *Pitx3 is required for development of substantia nigra dopaminergic neurons.* Proc Natl Acad Sci U S A, 2003. **100**(7): p. 4245-50.
37. Hwang, D.Y., et al., *Selective loss of dopaminergic neurons in the substantia nigra of Pitx3-deficient aphakia mice.* Brain Res Mol Brain Res, 2003. **114**(2): p. 123-31.

38. Ding, Y., et al., *Chronic 3,4-dihydroxyphenylalanine treatment induces dyskinesia in aphakia mice, a novel genetic model of Parkinson's disease.* Neurobiology of disease, 2007. **27**(1): p. 11-23.
39. Sinha, S. and J.K. Chen, *Purmorphamine activates the Hedgehog pathway by targeting Smoothened.* Nat Chem Biol, 2006. **2**(1): p. 29-30.
40. Pahwa, R., et al., *Amantadine extended release for levodopa-induced dyskinesia in Parkinson's disease (EASED Study).* Movement disorders : official journal of the Movement Disorder Society, 2015. **30**(6): p. 788-95.
41. Stanley, P., et al., *Meta-analysis of amantadine efficacy for improving preclinical research reliability.* Mov Disord, 2018. **33**(10): p. 1555-1557.
42. Taipale, J., et al., *Patched acts catalytically to suppress the activity of Smoothened.* Nature, 2002. **418**(6900): p. 892-7.
43. Marigo, V., et al., *Biochemical evidence that patched is the Hedgehog receptor.* Nature, 1996. **384**(6605): p. 176-9.
44. Guo, Q., et al., *Whole-brain mapping of inputs to projection neurons and cholinergic interneurons in the dorsal striatum.* PloS one, 2015. **10**(4): p. e0123381.
45. Whim, M.D. and P.E. Lloyd, *Frequency-dependent release of peptide cotransmitters from identified cholinergic motor neurons in Aplysia.* Proc Natl Acad Sci U S A, 1989. **86**(22): p. 9034-8.
46. Su, Y., et al., *High frequency stimulation induces sonic hedgehog release from hippocampal neurons.* Sci Rep, 2017. **7**: p. 43865.
47. Matamales, M., et al., *Aging-Related Dysfunction of Striatal Cholinergic Interneurons Produces Conflict in Action Selection.* Neuron, 2016. **90**(2): p. 362-73.
48. Matamales, M., J. Gotz, and J. Bertran-Gonzalez, *Quantitative Imaging of Cholinergic Interneurons Reveals a Distinctive Spatial Organization and a Functional Gradient across the Mouse Striatum.* PloS one, 2016. **11**(6): p. e0157682.
49. Bertran-Gonzalez, J., et al., *Striatal cholinergic interneurons display activity-related phosphorylation of ribosomal protein S6.* PloS one, 2012. **7**(12): p. e53195.
50. Seppi, K., et al., *Update on treatments for nonmotor symptoms of Parkinson's disease-an evidence-based medicine review.* Mov Disord, 2019. **34**(2): p. 180-198.
51. Voon, V., et al., *Impulse control disorders and levodopa-induced dyskinesias in Parkinson's disease: an update.* Lancet Neurol, 2017. **16**(3): p. 238-250.

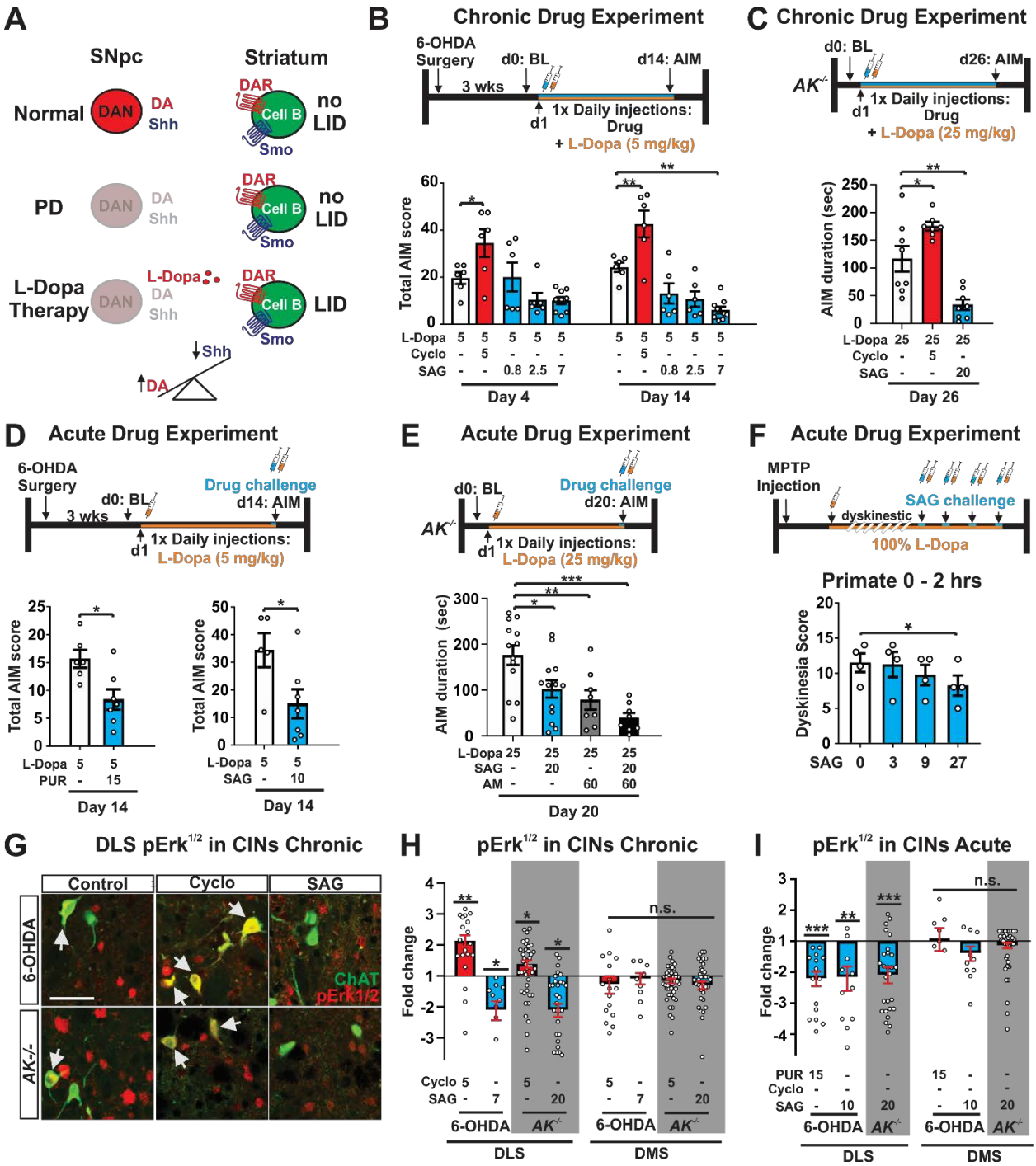

Figure 1: Smo inhibition facilitates while Smo stimulation attenuates LID in neurotoxic and genetic models of PD.

(A) DA substitution therapy without augmenting Shh signaling must lead to an imbalance of DA and Shh signaling onto CIN in the PD brain. **(B)** 6-OHDA chronic drug experiment (Cyclo (Cyclopamine) or SAG) and L-Dopa dosed daily for 14 days. AIM score (Method) with either vehicle (n = 6), Cyclo (5 mg/kg; n = 6), or SAG (7 mg/kg; n = 9). RM 2-way ANOVA treatment effect: $F_{(4,28)} = 12.24$, $p<0.0001$. Post hoc Bonferroni's test:* $P<0.05$, ** $P<0.01$ treatment vs. control. **(C)** *AK*$^{-/-}$ chronic drug experiment

(Cyclo, or SAG) and L-Dopa daily for 26 days. AIM duration (Method) with either vehicle (n = 7 - 8), Cyclo (5 mg/kg; n = 7), or SAG (20 mg/kg; n = 8). 1-way ANOVA $F_{(2,20)} = 20.46$ $p<0.0001$. Post hoc Bonferroni's test: * $P<0.05$, ** $P<0.01$ treatment vs. control. **(D)** 6-OHDA acute drug challenge (PUR (purmorphamine), or SAG) following chronic daily L-Dopa. AIM score with vehicle (n = 6) or PUR (15 mg/kg; n = 7; left) and AIM score with vehicle (n = 5) or SAG (10 mg/kg; n = 7; right). Unpaired 2-tailed student's t test * $P<0.05$ treatment vs. control. **(E)** AIM duration of *AK*$^{-/-}$ mice challenged with either vehicle (n = 13), Cyclo (5 mg/kg; n = 13), SAG (20 mg/kg; n = 13), AM (amantadine, 60 mg/kg; n = 8) or SAG combined with AM (n = 8). 1-way ANOVA $F_{(4,50)} = 9.79$ $p<0.0001$. Post hoc Bonferroni's test:* $P<0.05$, ** $P<0.01$, *** $P<0.001$ treatment vs. control. **(F)** Dyskinetic parkinsonian monkeys were generated over 7 months by 1-methyl-4-phenyl-1,2,3,6-tetrahydropyridine intoxication protocol followed by chronic L-Dopa treatment (Method). Once stabily dyskinetic , they were challenged with vehicle or SAG (3, 9, and 27 mg/kg) administered intravenously (i.v.) concomitant to oral L-Dopa in a within-subject drug escalation design (Method). Dyskinesia score binned for the first 2 hours (n = 4). Friedman's nonparametric RM 1-way ANOVA followed by Dunn's post hoc test *$P< 0.05$. **(G)** Representative images of pErk$^{1/2}$ (red) co-localization (arrowhead/yellow) with ChAT (green) in the DLS upon chronic drug dosing (Scale bar = 50 µm). **(H)** Quantification of the prevalence of pErk$^{1/2}$ positive CINs upon chronic drug dosing as fold change over vehicle in the DLS and DMS (~36 CINs per condition). Unpaired 2-tailed student's t test * $P<0.05$, ** $P<0.01$ treatment vs. vehicle. **(I)** Same as in (H) upon a single dose of SAG (~36 CINs per condition). Unpaired 2-tailed student's t test ** $P<0.01$, *** $P<0.001$, for treatment vs. vehicle. n.s. indicates $P > 0.05$. All bar graphs plotted as mean +/- SEM.

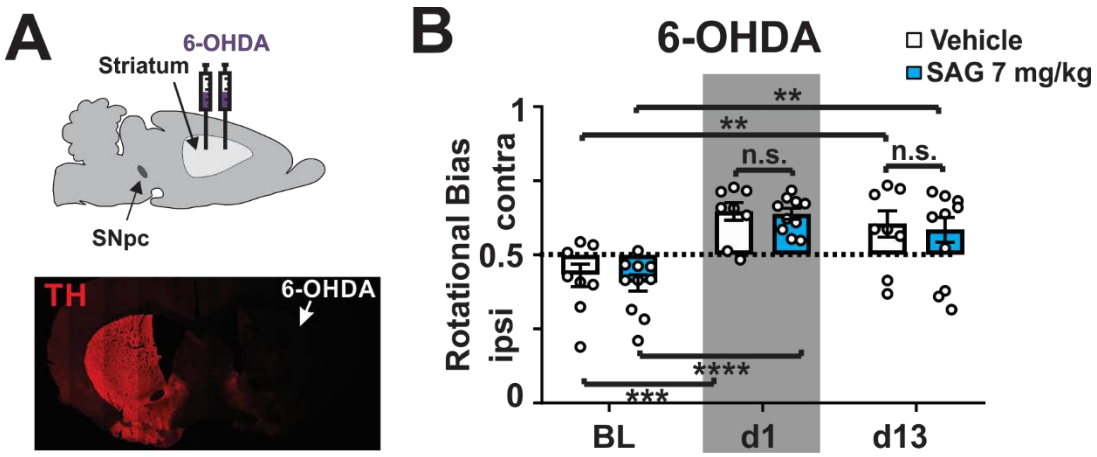

Extended Data Fig. 1: Histological and functional validation of the 6OHDA lesion model.

(A) Immunohistochemical staining of tyrosine hydroxylase (TH) in the striatum indicating unilateral loss of dopaminergic neuropil indicative of severe DAN lesion ipsilateral to striatal 6-OHDA injection. **(B)** Quantification of rotational bias calculated as contra- to ipsi- lateral turn ratio. Dotted line at 0.5 signify absence of turning bias. Mice with 6-OHDA lesions (baseline: BL) turn ipsilateral to the lesion. Upon L-dopa dosing 6OHDA lesioned mice turn contralateral towards the lesion, indicative of the anti-akinetic effect of L-Dopa. Long-term dosing with both L-Dopa (5 mg/kg) and the Smo agonist SAG (7 mg/kg) did not alter contralateral turning compared to controls (n = 8 - 9). RM 2-way ANOVA time effect: $F_{(2,50)} = 20.19$ $p<0.0001$. Post hoc Bonferroni's test: ** $P < 0.01$; *** $P < 0.001$ BL vs. day 1 or day 13.

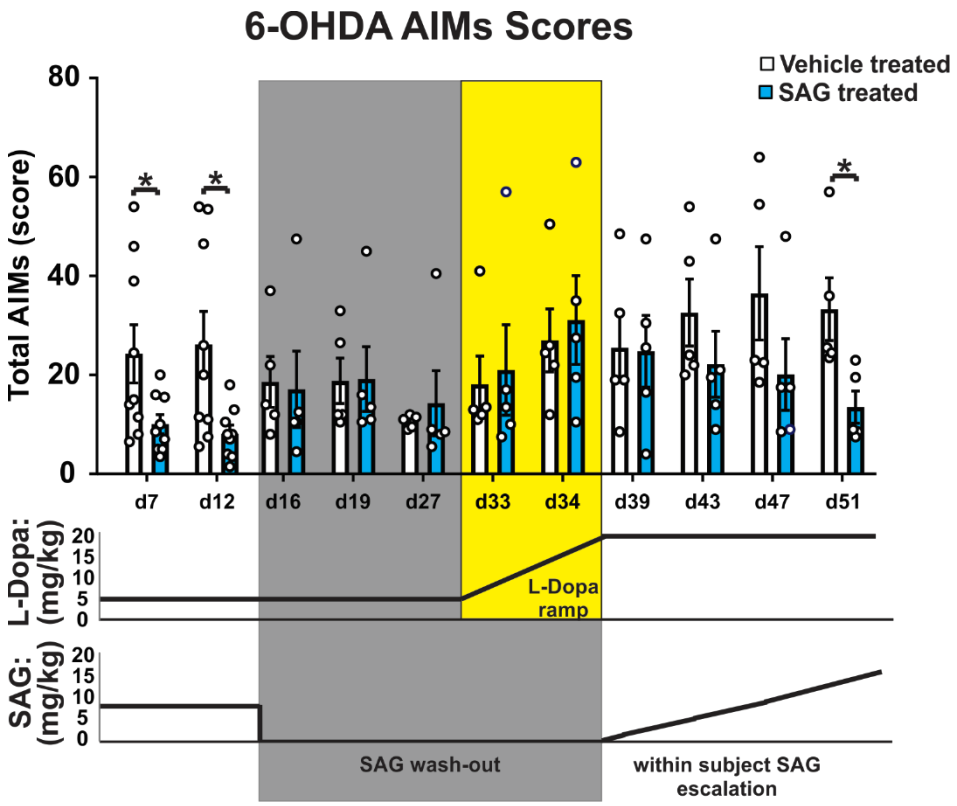

Extended Data Fig. 2: Reversibility study of Smo agonist mediated attenuation of LID in the 6OHDA lesion paradigm.

Daily dosing of 6-OHDA animals with L-Dopa together with the Smo agonist SAG (5 mg/kg) for 7 days resulted in significant attenuation of LID compared to L-Dopa only dosed controls. Additional days of co-administration of L-Dopa together with SAG did not further reduce LID. Terminating SAG while continuing L-Dopa treatment on day 16 resulted in an immediate reappearance of LID. Severity of reinstated LID remained sensitive to the L-Dopa concentration and could be intensified by gradual increased L-Dopa dosing with no difference in kinetics or absolute intensity compared to controls between days 33 – 51. Reinstated LID could be attenuated by a within subject escalation of SAG from days 39 - 51 from 1, 5, 10, and 15 mg/kg with 3 days of washout with only L-Dopa in between. (n = 9 for d 7, 12; n = 5 for d 16 – 51; Paired 2-tailed student's t test: * $P < 0.05$ treatment vs. vehicle. n.s. indicates $P > 0.05$. Bar graph plotted as mean +/- SEM.

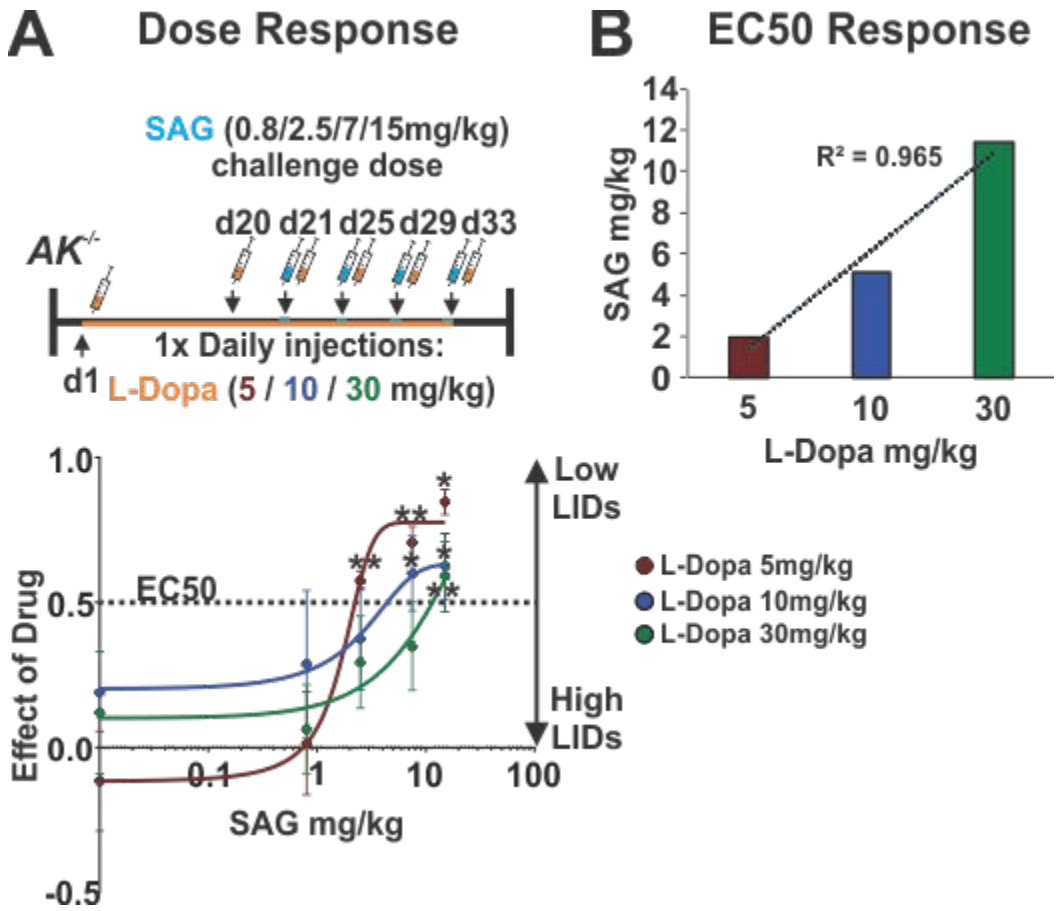

Extended Data Fig. 3: The dose of SAG needed to counteract LID co-varies with the dose of L-Dopa

The opposite effect of inhibition and stimulation of Smo signaling on LID under otherwise constant L-Dopa dosing suggests that the severity of LID may be correlated to the relative difference between Smo and DA signaling. Therefore, the dose-response relationship between L-Dopa and SAG was examined. **(A)** LID were induced in three separate groups of *AK*$^{-/-}$ mice, receiving either 5, 10 or 30 mg/kg of L-Dopa daily leading to distinct, concentration dependent, levels of AIMs severity. In a probe trial, the degree of LID attenuation was tested using four different concentrations of SAG 0.8; 2.5; 7.5; and 15 mg/kg in each L-Dopa group as a within subject escalation with 3 days of SAG washout in between each incremental SAG increase. **(B)** In each L-Dopa group, the attenuation of LID by SAG was dose-dependent. These results allowed the calculation of the estimated concentration of SAG that resulted in half-maximal (EC50) inhibition of LID in each of the three L-Dopa concentration groups. (Linear regression lines were plotted to best fit the data points. Stars represent significance to corresponding controls receiving L-Dopa and vehicle only. n = 8 for each drug condition; unpaired 2-tailed Student's t test * $P<0.05$, ** $P<0.01$**.** n.s. indicates $P > 0.05$. Graph plotted as mean +/- SEM.) **(C)** The analysis revealed a correlation between the dose of SAG needed to counteract AIMs that formed in response to escalating concentrations of L-Dopa compared to controls receiving only L-Dopa ($R^2 = 0.934$) These results indicate that the severity of LID is determined by the degree of imbalance between Shh/Smo- and DA- signaling.

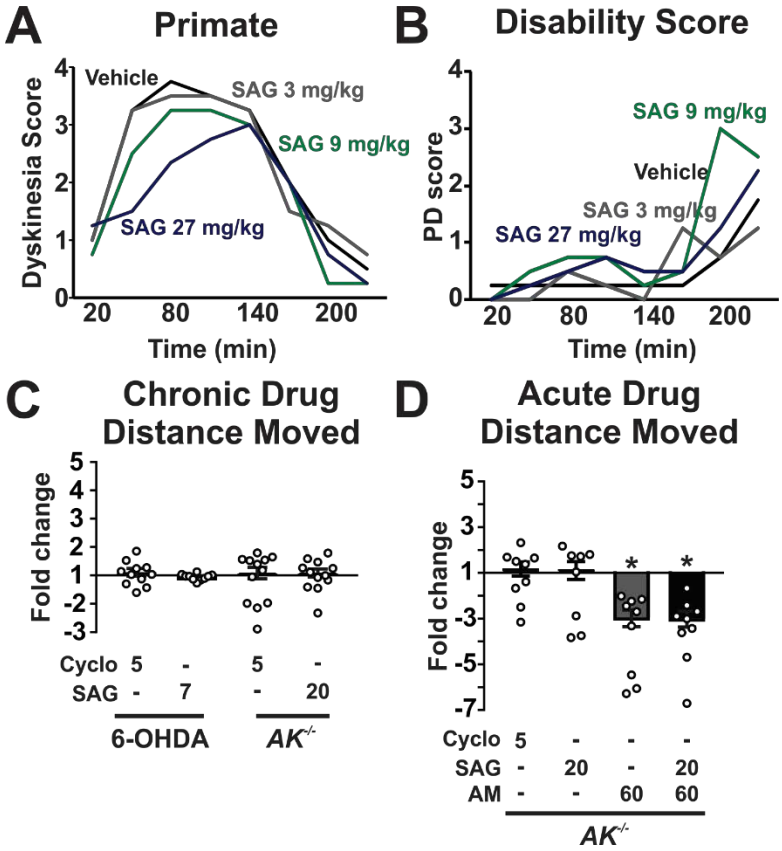

Extended data Fig. 4: Smo pharmacology does not dampen the anti-parkinsonian L-Dopa benefit.

(A) Time course of behavioral scores of dyskinesia over 4 hours for vehicle or SAG (3, 9, and 27 mg/kg). Error bars excluded for clarity. (n = 4)**. (B)** Time course of disability score of primates during L-Dopa treatment with either vehicle or SAG (3, 9, and 27 mg/kg) over 4 hours. Parkinson's Disease (PD) scoring consists of a range of movements including bradykinesia, postural abnormality, and tremor giving a maximum global parkinsonian disability score of 10. Error bars excluded for clarity. **(C)** Fold change of distance moved following chronic co-treatment of L-Dopa and either Cyclo or SAG in 6-OHDA- (day 14; n = 8) and *AK*$^{-/-}$ - (day 26; n = 12) mice over L-Dopa and vehicle treated controls. **(D)** Fold change of distance moved on day 20 following chronic L-Dopa and acute treatment in *AK*$^{-/-}$ mice following 5 mg/kg Cyclo (n = 9), 20 mg/kg SAG (n = 8), 60 mg/kg Amantadine (AM; n=9), or combined AM and SAG (n = 8). Amantadine, but not SAG, reduced significantly the anti-akinetic benefit of L-Dopa. (Unpaired 2-tailed student's t test: * $P < 0.05$ for treatment vs. vehicle. n.s. indicates $P > 0.05$. All bar graphs plotted as mean +/- SEM.)

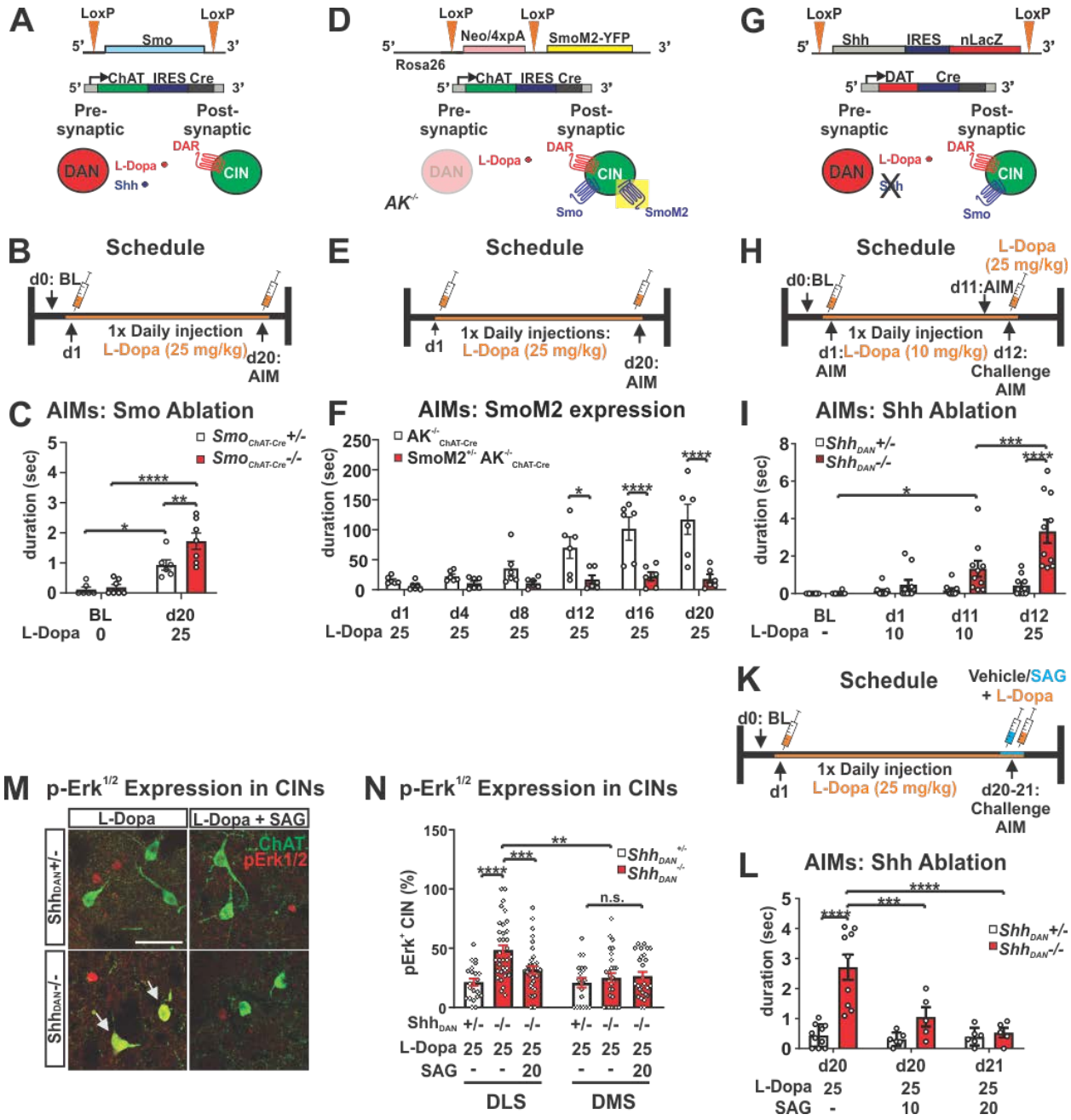

Figure 2: Signaling of Shh_{DAN} to Smo on CIN of the DLS protects from LID. (A) Smo was selectively ablated from cholinergic neurons by ChAT-IRESCre (Method). **(B)** L-Dopa dosing schedule for Smo loss of function study. **(C)** $Smo_{ChAT\text{-}cre}^{-/-}$ mice developed AIMs in response to daily injection of 25 mg/kg L-Dopa for 20 days (n = 6–7 per genotype; RM 2-way ANOVA day x genotype effect: $F_{(1,11)}$ 4.95, p=0.048. Post hoc Bonferroni's test: ** P<0.01 control vs. mutant on d20; and day effect: $F_{(1,11)} = 52.61$, p<0.0001; * P<0.05 control BL vs. d20 and **** P<0.0001 mutant BL vs. d20). **(D)** SmoM2 was selectively expressed in cholinergic neurons by ChAT-IRESCre in $AK^{-/-}$ mice (Method). **(E)** L-Dopa dosing schedule for SmoM2 gain of function study. **(F)** SmoM2 expressed in cholinergic neurons in $AK^{-/-}$ mice ($SmoM2^{+/-}AK^{-/-}{}_{ChAT\text{-}Cre}$) blocked AIMs that form in LID-prone $AK^{-/-}$ controls ($AK^{-/-}{}_{ChAT\text{-}Cre}$) in

response to daily injection of 25 mg/kg L-Dopa for 20 days (n = 6 per genotype; RM 2-way ANOVA time x genotype effect: $F_{(5,50)}$ =8.16, p=<0.0001. Post hoc Bonferroni's test: * P<0.05, **** P<0.0001 control vs. mutant). **(G)** Shh was selectively ablated from DAN by Dat-Cre (Method). **(H)** L-Dopa dosing schedule for Shh loss of function study. **(I)** $Shh_{DAN}^{-/-}$ mutants but not $Shh_{DAN}^{-/+}$ controls developed AIMs in response to daily injection of 10 mg/kg L-Dopa for 11 days (RM 2-way ANOVA day x genotype: $F_{(2,36)}$ = 4.53, p=0.018. Post hoc Bonferroni's test: * P<0.05 for BL vs. d11). Severity of AIMs increased in response to a 25 mg/kg L-Dopa challenge on Day 12 (RM 2-way ANOVA treatment effect: $F_{(1,18)}$ = 16.23, p=0.001. Post hoc Bonferroni's test: *** P<0.001 d11 vs. d12; genotype effect: $F_{(1,18)}$ = 18.36, p=0.0004. Post hoc Bonferroni's test: **** P<0.0001 control vs. mutant on d12; n = 10 per genotype). **(K)** L-Dopa and SAG dosing schedule for the pharmacological complementation of the LID phenotype seen in $Shh_{DAN}^{-/-}$ mutants. **(L)** Dosing with 10 or 20 mg/kg SAG attenuated AIMs dose dependently in $Shh_{DAN}^{-/-}$ mutants but had no effect in controls. (n = 5 - 10; 2-way ANOVA genotype effect: $F_{(1,35)}$ = 21.36, p=0.0002. Post hoc Bonferroni's test: **** P<0.0001 control vs. mutant on d 20; genotype x treatment effect: $F_{(2,35)}$=9.15, p=0.001. Post hoc Bonferroni's test:*** P<0.001, **** P<0.0001 mutant with and without SAG on d 20 and d 21. **(M)** Representative images of $pErk^{1/2}$ (red) co-localization (arrowhead/yellow) with ChAT (green) in the DLS of $Shh_{DAN}^{-/-}$ mutants and $Shh_{DAN}^{-/+}$ controls upon chronic daily L-Dopa alone or L-Dopa with SAG dosing (Scale bar = 50 µm). **(N)** Quantification of the prevalence of $pErk^{1/2}$ positive CIN in (M). (n = 8 - 12, 35-38 CINs per genotype and drug condition; 3-way ANOVA genotype effect: $F_{(1,105)}$ = 7.093, p=0.01. Post hoc Bonferroni's test: **** P<0.0001 control vs. mutant; treatment effect: $F_{(1,105)}$ = 9.79, p=0.002. Post hoc Bonferroni's test: **** P<0.0001 mutant with and without SAG; Area x genotype: $F_{(1,98)}$ = 11.21, p=0.001. Post hoc Bonferroni's test: **P<0.01 mutant DLS vs. DMS. All bar graphs plotted as mean +/- SEM.

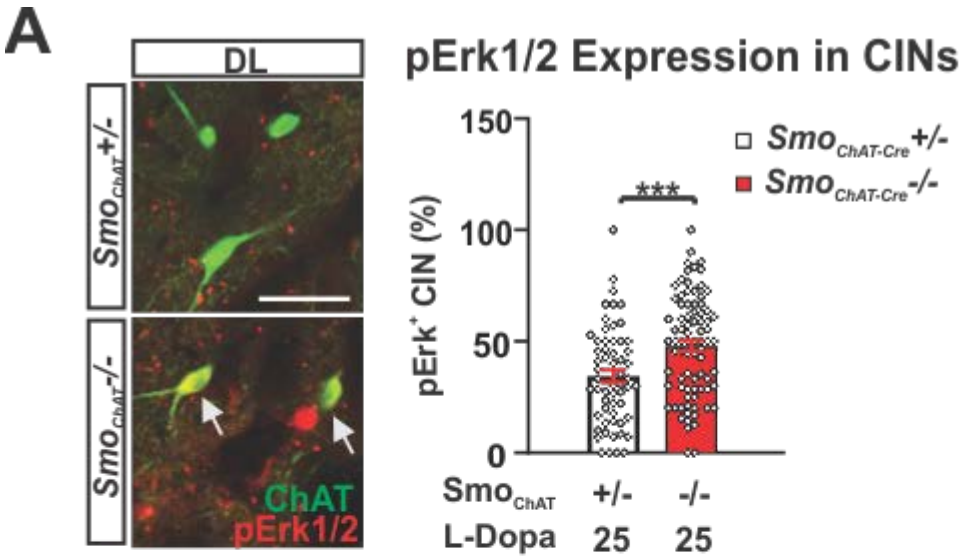

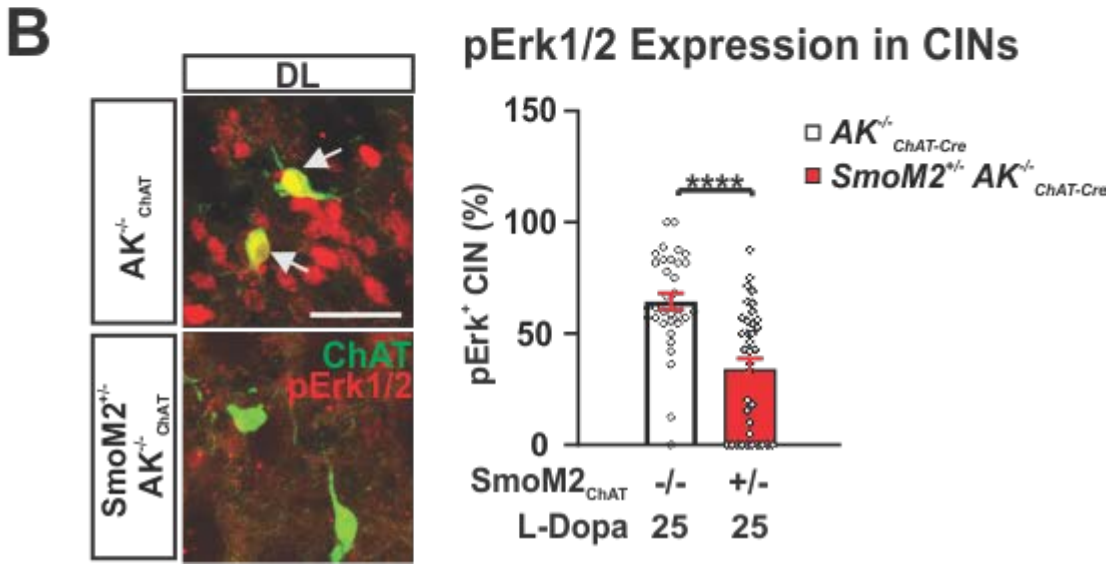

Extended data Fig. 5: Bi-directional effect on prevalence of pErk$^{1/2}$ positive CIN in the DLS following either Smo ablation or SmoM2 expression in CIN

(A) Representative images of pErk$^{1/2}$ (red) co-localization (yellow, white arrows) in CIN (ChAT, green) following 25 mg/kg L-Dopa in the DL striatum (Scale bar = 50µm). Quantification of percent of pErk$^{1/2+}$ CINs (n = 6 – 7 per genotype, 35-38 CIN each). Unpaired 2-tailed student's t test *** P<0.001 control vs. mutant. **(B)** Representative images of pErk$^{1/2}$ (red) co-localization (yellow, white arrows) in CIN (ChAT, green) following 25 mg/kg L-Dopa in the DL striatum (Scale bar = 50 µm). Percent of pErk$^{1/2}$ positive CINs (n = 8 - 12, 35 - 38 CINs each). Unpaired 2-tailed student's t test **** P<0.0001 control vs. mutant**.** All bar graphs plotted as mean +/- SEM.

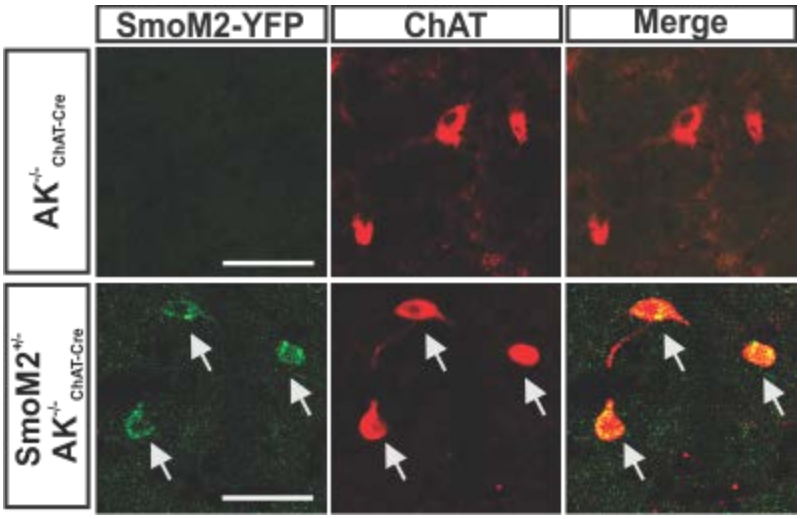

Extended data Fig. 6: SmoM2 allele is expressed in CIN in AK-/- mice.

Images of the DLS showing recombination of constitutively active version SmoM2 specifically in CINs using eYFP (green, Method) co-labeled with ChAT (red, white arrows) that is not seen in $AK^{-/-}{}_{ChAT\text{-}Cre}$ control mice.

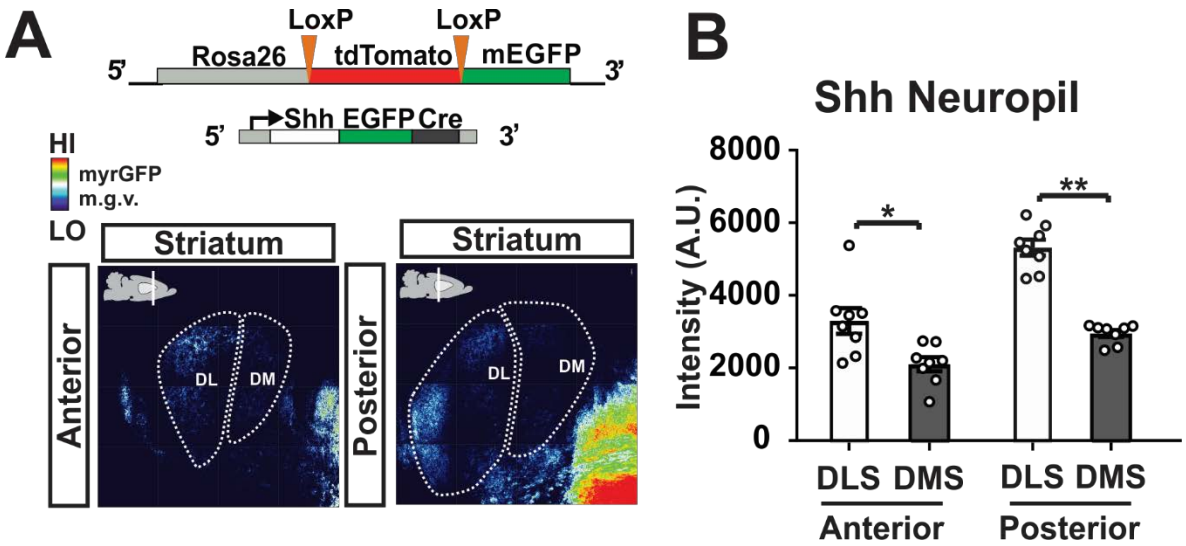

Extended Data Figure 7: Shh signaling is patterned in the dorsal striatum

(A) Conditional activation of myristylated GFP (mGFP) expression by Shh-Cre (Method) reveals a stereotypic greater density of Shh carrying neurites in the DLS compared to the DMS shown as heat map based on a 16 member pseudocolor palette to depict fluorescence intensity. **(B)** Quantification based on the mean gray value intensity (m.g.v.) of Shh carrying neurites in the anterior and posterior DLS and DMS (n=8; paired 2-tailed student's t test * $P<0.05$ and ** $P<0.01$ DLS vs. DMS).

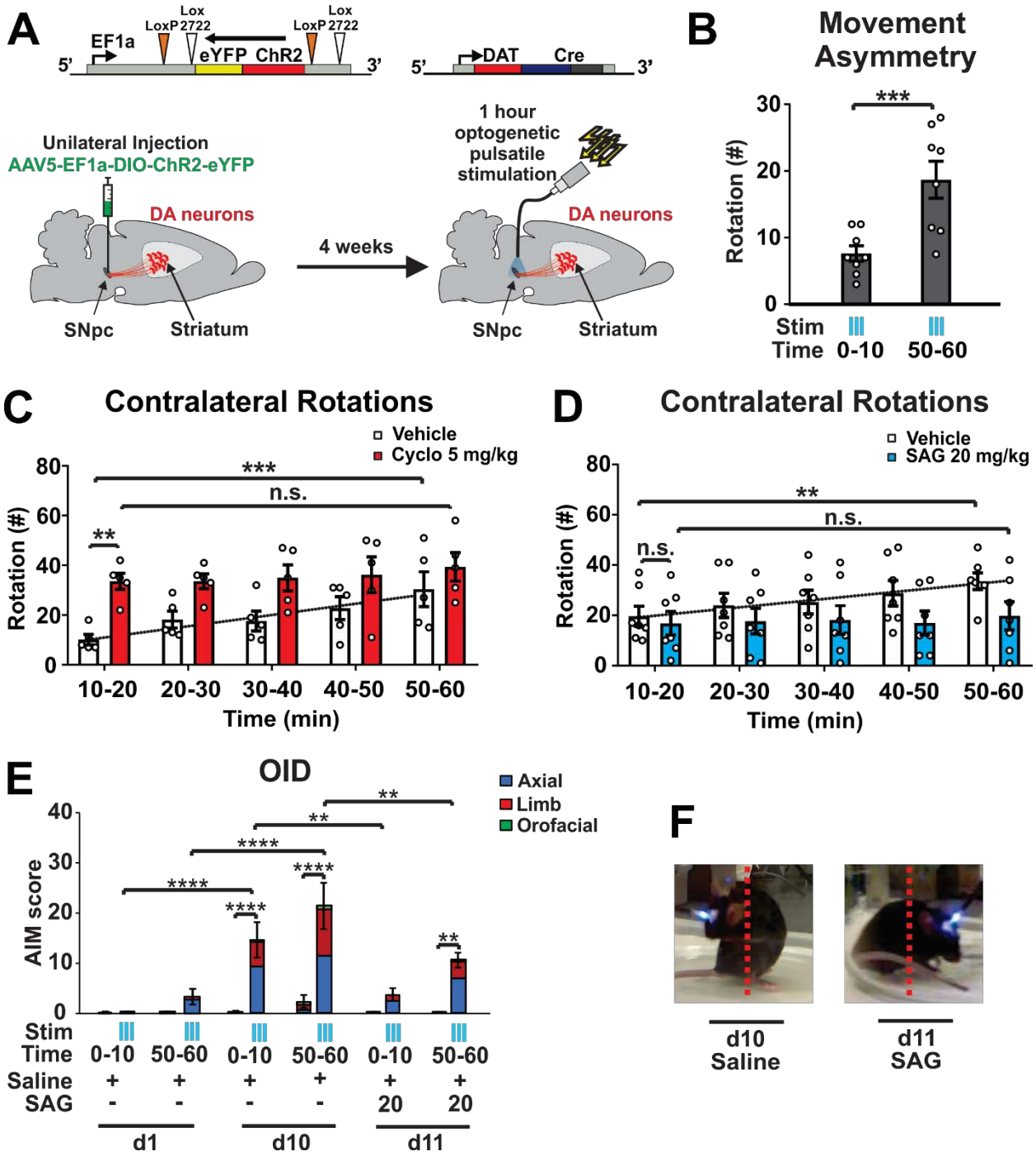

Figure 3: Optical stimulation of DAN exhausts Shh_{DAN} leading to AIMS that can be attenuated by Smo agonist treatment.

(A) Channelrhodopsin was expressed unilateral in DAN of the ventral midbrain, which were subsequently stimulated with 5 sec of 10 msec long pulses at 60 Hz followed by a 30 sec pause for one hour per day during which AIMs were scored. **(B)** Contralateral rotations intensified during DAN stimulation sessions (n = 8; paired 2-tailed Student's t test ***P<0.001). **(C)** Number of contralateral rotations in 10 min bins over the course of an hour of stimulation in animals injected with vehicle or Cyclo (n = 5 per condition; RM 2-way ANOVA treatment effect: $F_{(1,8)}$= 7.40 p=0.026. Post hoc Bonferroni's test: **P<0.01 vehicle

(veh) vs. cyclopamine (Cyclo); time effect $F_{(4,32)}$= 5.69 p=0.001. Post hoc Bonferroni's test: ***P<0.001 veh 10-20 min vs. veh 50-60 min). **(D)** Contralateral rotations as in (C) following vehicle or SAG (n = 7 per condition; RM 2-way ANOVA time effect: $F_{(4,44)}$= 6.96 p=0.0002. Post hoc Bonferroni's test: **P<0.01 veh 10-20 min vs. veh 50-60 min). **(E)** Axial (red), limb (green), and orofacial (yellow) AIMs scored during off stimulation and on stimulation (blue ticks) in the first 10 and last 10 mins for day 1, 10 and 11 (n = 8; 2-way ANOVA stimulation effect: $F_{(1,38)}$ = 61.1 p<0.0001. Post hoc Bonferroni's test: **** P<0.0001 stimulation vs. non-stimulation d10, and **P<0.01 stimulation vs. non-stimulation d11; time x stimulation effect: $F_{(15,38)}$ = 8.59 p<0.0001. Post hoc Bonferroni's test: **** P<0.0001 stimulation during d1 vs. d10, and **P<0.01 stimulation during d10 vs. d11)**.** **(F)** Video still images of mouse posture during stimulation showing axial AIM on day 10 which is not present on day 11 following SAG treatment (extended data video feeds online).

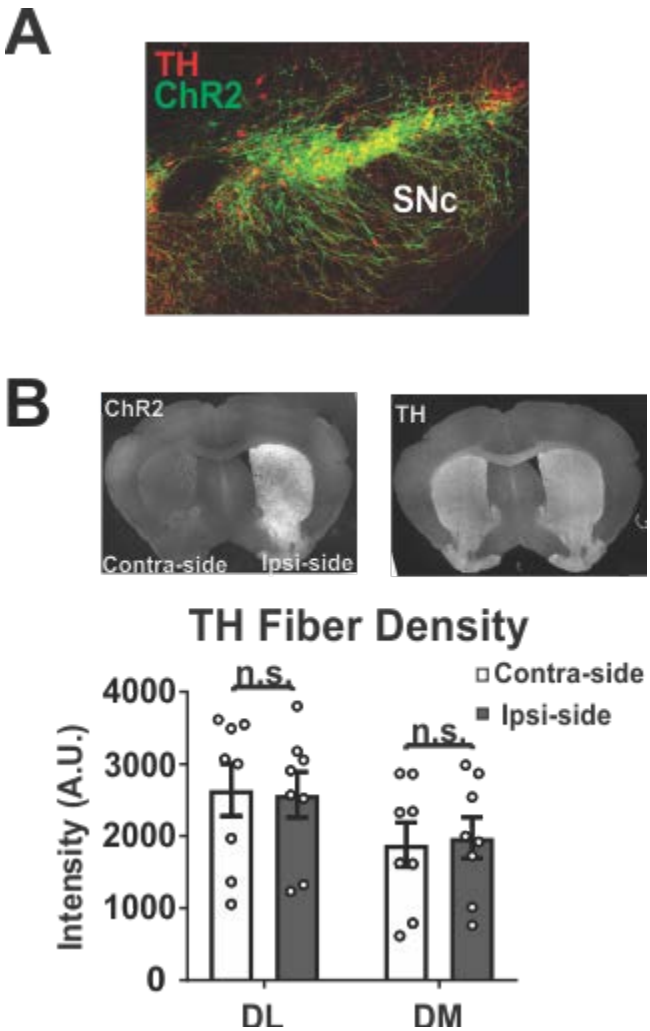

Extended Data Fig. 8: Long term optogenetic stimulation of DAN does not alter dopaminergic fiber density in the striatum.

(A) eYFP (green), bi-cistronically expressed together with channelrhodopsin (ChR2) upon Cre recombination is co-localized with TH (red) in the SNpc. **(B)** Representative images and quantification revealing that unilateral expression of ChR2 and prolonged optogenetic stimulation does not alter TH fiber density in the ipsilateral striatum compared to the contralateral hemisphere (n = 8; n.s. indicates P > 0.05).

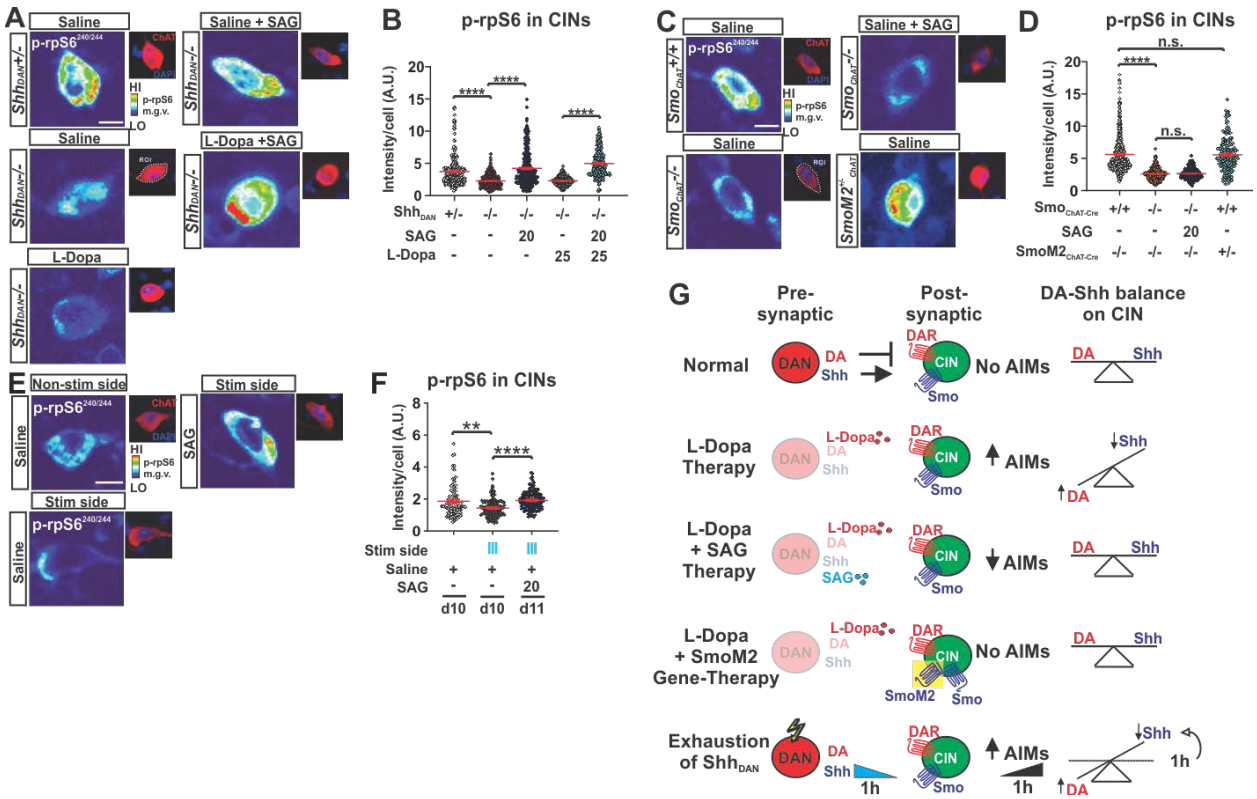

Figure 4: Effect of Shh/Smo signaling on p-rpS6$^{240/244}$ levels in CIN of the dorsolateral striatum.

(A) Representative heat mapped expression levels of p-rpS6$^{240/244}$ in CIN of the DLS in *Shh$_{DAN}$-/-* mutants and controls and in response to L-Dopa (25 mg/kg) and SAG (20 mg/kg; Scale bar = 10 µm). p-rpS6$^{240/244}$ levels were normalized to NeuN in identified CIN (ChAT staining, smaller images; Method). **(B)** Ablation of Shh from DAN resulted in depressed levels of p-rpS6$^{240/244}$ in CIN that could be normalized by SAG alone or in the presence of L-Dopa. (n = 3-4 per genotype and drug condition, 60-100 cells per n; each dot represents one neuron; red lines indicate the mean ± SEM; Kruskal-Wallis nonparametric 1-way ANOVA followed by Dunn's post-test shows **** P<0.0001 controls vs. mutants, or mutants with and without treatment, n.s. indicates P > 0.05.) **(C)** Representative heat mapped expression levels of p-rpS6$^{240/244}$ in CIN of the DLS in *Smo* loss or gain of function mutants and in response to SAG (20 mg/kg; Scale bar = 10 µm). **(D)** Ablation of Smo from CIN resulted in depressed levels of p-rpS6$^{240/244}$ in CIN that could not be normalized by SAG (n = 3-4 per genotype and treatment group, 60-100 cells per n; Kruskal-Wallis nonparametric 1-way ANOVA followed by Dunn's post-test shows **** P<0.0001 controls vs. mutants, or mutants with and without SAG, n.s. indicates P > 0.05). **E)** Representative heat mapped expression levels of p-rpS6$^{240/244}$ in CIN of the DLS in response to optogenetic stimulation of DAN (Scale bar = 10 µm) and **(F)** One hour of pulsatile stimulation diminished p-rpS6$^{240/244}$ levels in CIN that could be normalized by SAG treatment prior to stimulation onset (n = 2 per saline and n = 6 for SAG, 40 to 100 cells per n; paired 2-tailed Student's t test ** P<0.01 stimulated (stim) vs. unstimulated side; Unpaired 2-tailed Student's t test ****P<0.0001 saline vs. SAG). **(G)** Summary: Consistent across established models of PD, pre and post synaptic loss and gain of function Shh/Smo signaling between DAN and CIN and graded exhaustion of Shh$_{DAN}$, our data indicates that diminishment of Shh/Smo signaling onto CIN facilitates AIMs while boosting Shh/Smo signaling attenuates AIMs.

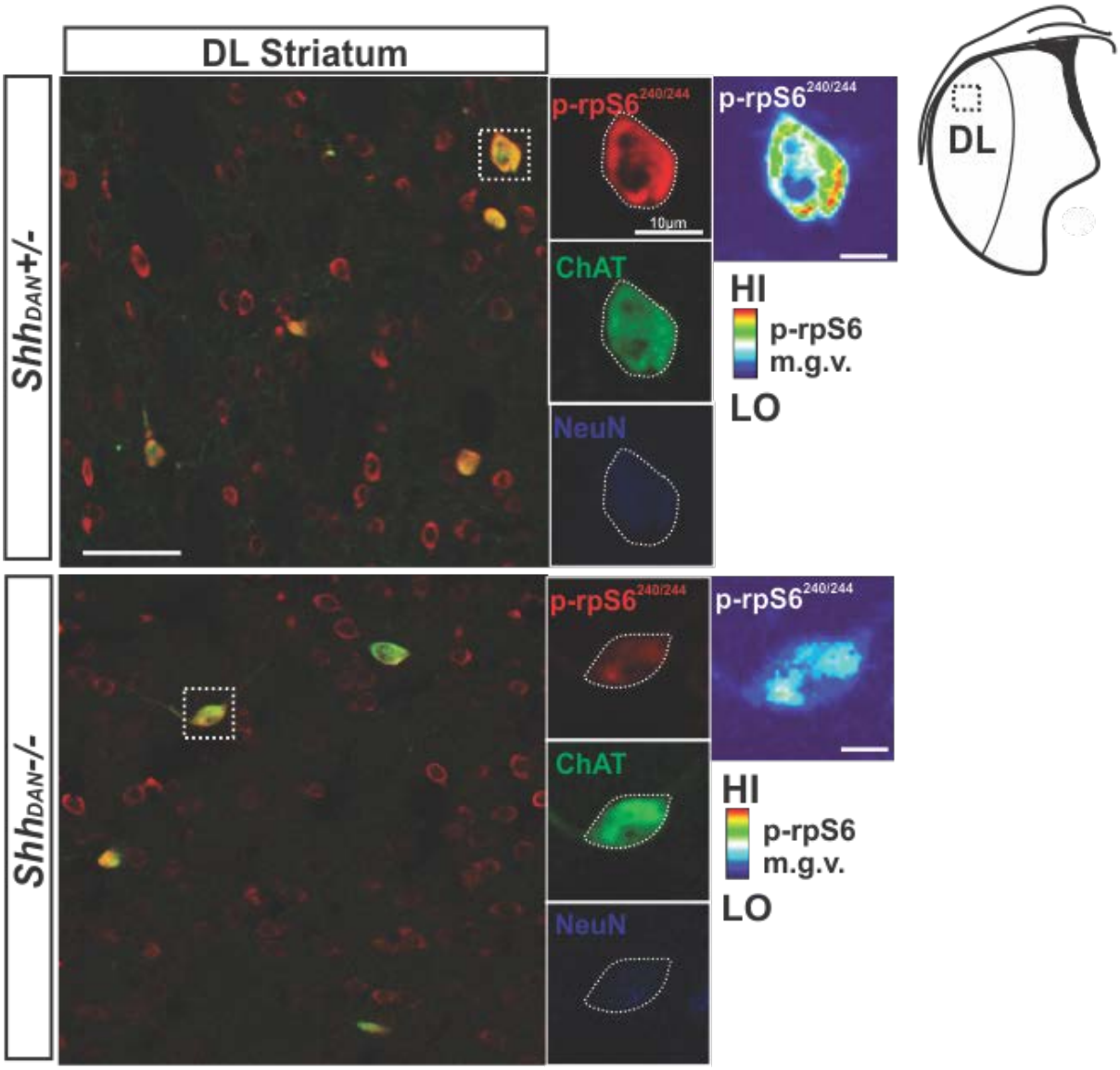

Extended data Fig. 9: Detection and normalization of neuronal activity marker p-rpS6$^{240/244}$ expression in CINs

Large 20x raw images showing p-rpS6$^{240/244}$ co-localized in CINs for basal levels of *Shh*$_{DAN}^{+/-}$ mice (top), *Shh*$_{DAN}^{-/-}$ mice (bottom; Scale bar = 50 µm). Smaller panels show zoomed in image of square (Scale bar = 10 µm) with markers for p-rpS6$^{240/244}$ (red), ChAT (green), NeuN (blue) and a heat map of p-rpS6 showing a 16 member pseudocolor palette to depict the intensity of p-rpS6$^{240/244}$ fluorescence. Left scheme shows the DLS where the images were taken from.

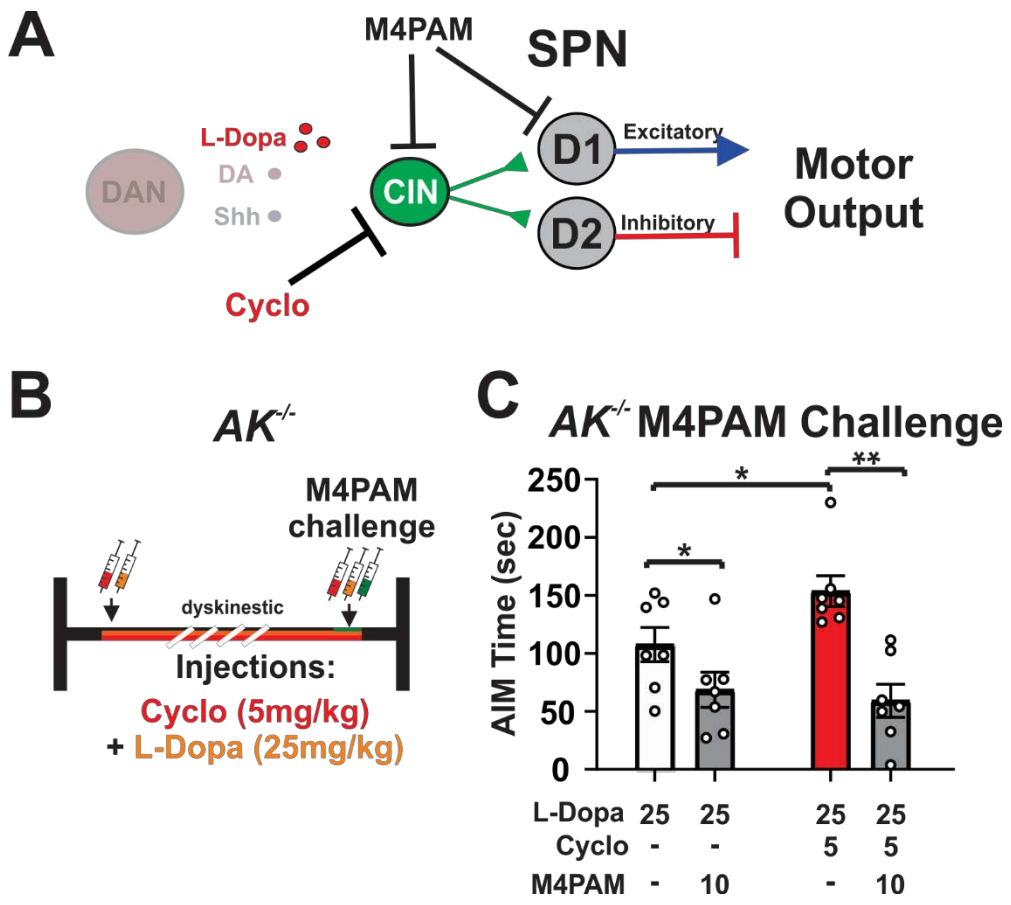

Extended Data Figure 10: Shh/Smo signaling reduces AIMs by acting upstream of striatal output pathways.

(A) The muscarinic receptor 4 positive allosteric modulator (M4PAM) attenuates AIMs by boosting cholinergic signaling onto D1 receptor positive medium spiny projection neurons (DR1-MSN) of the striatum where it facilitates long term depression (LTD) [16]. This observation is concordant with our finding that increased levels of the activity marker **p-rpS6$^{240/244}$** in CIN correlate with reduced AIMs (Fig. 4). The inhibition of LID by M4PAM afforded us test whether the Smo mediated modulation of AIMs in *AK*$^{-/-}$ mice is upstream or downstream of the action of M4PAM on DR1-MSN. We found that the Cyclo induced increase in AIMs can be attenuated by M4PAM to the same levels achieved by M4PAM in L-Dopa only treated *AK*$^{-/-}$ mice consistent with Smo mediated modulation of AIMs occurring presynaptic to M4 signaling on DR1-MSN. **(B)** Dosing schedule of *AK*$^{-/-}$ mice with L-Dopa (25 mg/kg) alone or L-Dopa (25 mg/kg) with Cyclo (5 mg/kg) until AIMs were established. Mice were then challenged with a single dose of M4PAM VU0467154 (10mg/kg) alone or in combination with Cyclo (5mg/kg). **(C)** AIM duration of *AK*$^{-/-}$ mice following daily L-Dopa dosing with either vehicle (veh) or Cyclo and challenged with M4PAM (n = 7). Paired 2-tailed Student's t test P<0.05, * P<0.05, ** P<0.01 veh vs. M4PAM. Unpaired 2-tailed Student's t test P<0.05, * P<0.05 veh vs. Cyclo. Bar graph plotted as mean +/- SEM.

16 Shen, W., et al., *M4 Muscarinic Receptor Signaling Ameliorates Striatal Plasticity Deficits in Models of L-DOPA-Induced Dyskinesia.* Neuron, 2016. **90**(5): p. 1139.

Methods:

Mice

All mice were maintained on a 12 h light/dark cycle, with ad libitum food and water. Animal use and procedures were in accordance with the National Institutes of Health guidelines and approved by the Institutional Animal Care and Use Committees (IACUC) of the City University of New York. All experiments were carried out in young adult animals beginning at 2 months of age and weighing between 22 – 28 g unless stated otherwise. Males and females from a mixed CD1 and C57/BL6 background were used for all experiments in approximately equal proportions.

C57/Bl6 mice, JAX # 000664, were purchased from Jackson Laboratory.

$AK^{-/-}$ mice are homozygous $Pitx3^{ak/ak}$ mice and were generously provided by Dr. Un Jung Kang (Columbia University), propagated by homozygous breeding and genotyped as previously described in [1, 2]).

$Shh_{DAN}^{-/-}$ mice and controls are produced by crossing Shh-nLacZ$^{L/L}$ females with Shh-nLacZ$^{L/+}$/DatCre males resulting in Shh-nLacZ$^{L/L}$/Dat-Cre experimental ($Shh_{DAN}^{-/-}$) - and Shh-nLacZ$^{L/+}$/Dat-Cre control ($Shh_{DAN}^{-/+}$) – mice as previously described in [3].

$Smo_{ChAT\text{-}Cre}^{-/-}$ mice and controls are produced by crossing Smo$^{L/L}$ females with Smo$^{L/+}$ /ChAT-IRES-Cre males resulting in Smo$^{L/L}$ /ChAT-IRES-Cre ($Smo_{CIN}^{-/-}$) experimental – and Smo$^{L/+}$ /ChAT-IRES-Cre ($Smo_{ChAT\text{-}Cre}^{-/+}$) control - mice. Smo L/+ (JAX # 004526; [4]) and ChAT-IRES-Cre (JAX # 006410; [5] mice were purchased from Jackson Laboratory.

$SmoM2^{+/-}{}_{ChAT\text{-}Cre}\ AK^{-/-}$ mice are ^{L}STOP^{L}SmoM2-YFP/ChAT-IRES-Cre /Pitx3$^{ak/ak}$ mice and are maintained by crossing Pitx3$^{ak/ak}$ females with triple heterozygous ^{L}STOP^{L}SmoM2-YFP/ChAT-IRES-Cre /Pitx3$^{ak/+}$ males resulting in ^{L}STOP^{L}SmoM2-YFP/ChAT-IRES-Cre /Pitx3$^{ak/ak}$ ($SmoM2^{+/-}{}_{ChAT\text{-}Cre}\ AK^{-/-}$) experimental – and ChAT-IRES-Cre /Pitx3$^{ak/ak}$ ($_{ChAT\text{-}Cre}\ AK^{-/-}$) – control mice. Tissue specific activation of SmoM2 was confirmed by eYFP expression. ^{L}STOP^{L}SmoM2-YFP mice (JAX # 005130; [6]) were purchased from Jackson Laboratory.

For the visualization of Shh carrying neuropil, Shh-Cre eGFP mice (JAX # 005622; [7]) were crossed with Rosa26mTmG (JAX # 007576; [8] to produce double heterozygous animals that express myristylated GFP in Shh expressing cells.

Genotyping

Gene	**Oligo Forward**	**Oligo Reverse**
Shh$^{fl/fl}$	GTAAGAGCACATTACCCAGAGAACTG	CCTGTTGTTACTGGATCCCTTCCATC
Cre	TAGCGCCGTAAATCAATCG	AATGCTTCTGTCCGTTTGC
Smo$^{fl/fl}$	ATGGCCGCTGGCCGCCCCGTG	GGCGCTACCGGTGGATGTGG
Smo WT	CCACTGCGAGCCTTTGCGCTAC	CCCATCACCTCCGCGTCGCA
SmoM2 Mutant	CTGACCCTGAAGTTCATCTGC	GTGCGCTCCTGGACGTAG
SmoM2 WT	CGTGATCTGCAACTCCAGTC	GGAGCGGGAGAAATGGATATG
ChAT-Cre	CAGGGTTAGTAGGGGCTGAC	CAAAAGCGCTCTGAAGTTCCT

ROSA26	CTCTTCCCTCGTGATCTGCAACTCC	CATGTCTTTAATCTACCTCGATGG
LacZ	GTCAATCCGCCGTTTGTTCCCACG	GCGTGTACCACAGCGGATGGTTCG
R26-L-Tomato-L-mGFP	CGAGGCGGATCACAAGCAATA	CTCTGCTGCCTCCTGGCTTCT

Macaques

The non-human primate experiments were performed in accordance with the European Union directive of September 22, 2010 (2010/63/EU) on the protection of animals used for scientific purposes in an AAALAC-accredited facility following acceptance of study design by the Institute of Lab Animal Science (Chinese Academy of Science, Beijing, China). The four Macaca fascicularis male monkeys (Xierxin, Beijing, PR of China) were housed in individual cages allowing visual contacts and interactions with other monkeys in adjacent cages. Food and water were available *ad libitum.* Animal care was supervised daily by veterinarians skilled in the healthcare and maintenance of NHPs.

Antibodies

Anti- tyrosine hydroxylase (1:500; RRID: AB_657012), anti-β Galactosidase (1:500; RRID: AB_986), and anti-ChAT (1:100; RRID: AB_144P) were purchased from Milipore. Anti-phospho-Erk1/2 (1:400; RRID: AB_9101), and anti-phospho-rpS6 (ser240/244; RRID: AB_5364) were from Cell Signaling Technology. Anti-NeuN (1:200; RRID: AB_MAB377) from Chemicon International. Various Alexa Fluor antibodies were used at 1:250 dilutions for immunohistochemistry (Jackson Immuno Research).

Drugs

In mice, all pharmacological agents were administered intraperitoneal (i.p.). Animals were treated daily in a volume of 10 mL/kg of body weight with a combination of L-Dopa (5-25 mg/kg; Sigma-Aldrich D1507) and the peripheral L-amino acid decarboxylase antagonist, benserazide (12.5-20 mg/kg; Sigma-Aldrich B7283) diluted in 0.9% sterile saline (referred to as just "L-Dopa" and specified doses described in main text). Sonic Hedgehog agonist (SAG Carbosynth Limited FS27779; 0.8-20 mg/kg) and antagonist (Cyclopamine Carbosynth Limited FC20718; 2.5-5 mg/kg) were dissolved in DMSO and brought into solution with 45% HPCD (Sigma Aldrich H107) in 0.9% sterile saline for 6-OHDA and $AK^{-/-}$ AIM studies. SAG-HCl (Carbosynth Limited FS76762) was diluted in 0.9% sterile saline and used for the $Shh_{DAN}^{-/-}$ and $Smo_{CIN}^{-/-}$ mouse studies. Both cyclopamine and SAG were administered 15 minutes before L-Dopa injections. Amantadine hydrochloride (Sigma Aldrich A1260) was dissolved in 0.9% sterile saline and given 100 minutes prior to L-Dopa administration. M4PAM (VU0467154 StressMarq Biosciences SIH184) was dissolved in 0.9% sterile saline and given at the same time as L-Dopa. Purmorphamine (ABCam AB120933) was dissolved in a cocktail of Polyethylene glycol (PEG) and ethanol in PBS and given 15 minutes before L-Dopa dosing. Control mice were treated with carrier (DMSO, HPCD etc.) in similar proportions to the treatment drugs.

Mouse unilateral 6-OHDA model [9].

Mice were anesthetized with a mixture of ketamine (80 mg/kg) and xylazine (12 mg/kg) administered i.p. and the surgical field was prepared with betadine. Bupivacaine (Marcaine Sigma Aldrich B5274), a local anesthetic, was subcutaneously (s.c.) injected near the incision site. Bregma was visualized with 3% hydrogen peroxide. There were two unilateral injections (2 x 2 µl each) of 6-OHDA into the left striatum using the following coordinates based on the Mouse Brain Atlas by Paxinos and Franklin (2001): Anteroposterior (AP) +1.0 mm; Lateral (ML), + 2.1 mm; Dorsoventral (DV), -2.9 mm; and AP +0.3 mm; L +2.4 mm; DV -2.9 mm. 6-OHDA-HCl (Sigma Aldrich H4381; 3.0 mg/ml) was dissolved in a solution containing 0.2 g/L ascorbic acid (Sigma Aldrich A92902) and 9 g/L NaCl and injected via a Hamilton syringe with a 33-gauge needle attached to a micro-syringe pump (World Precision Instruments) at a rate of 0.4 µl/min and left in place for 3 minutes and then retracted slowly. Following surgery, animals were injected with 5% sucrose (10 ml/kg, s.c.) and saline (10 ml/kg, i.p.) and recovered on a heating pad. To avoid dehydration and weight loss, hydrogel pouches and hi-fat chow were given to the mice ad lib. Behavioral testing and drug treatment began three weeks following surgery. Lesion assessments were quantified by ipsilateral paw-use bias in the cylinder test and verified histologically, post-mortem, by quantification of tyrosine hydroxylase (TH) fiber density at the end of experiments. Only animals with 70% or more of TH positive fiber depletion were included in the analyses.

Forelimb cylinder test

The cylinder test was used to assess the anti-akinetic effects of L-Dopa for the 6-OHDA lesioned mice by measuring forelimb paw placement. Mice were placed in a glass cylinder (10 cm wide x 14 cm high) 30 minutes post L-Dopa injection and analyzed for 4 minutes. Two mirrors were placed in the back to observe mice from all angles. The limb use asymmetry score was expressed as a ratio of contralateral to the lesion paw use over the total number of wall contacts with both paws as described previously in [10].

Open field test

In the open field test (OFT), whole body movements were measured for 5 min using a Noldus Ethovision XT video tracking system. The animals head, body, and tail positions were tracked in a transparent Plexiglas 4-chamber box apparatus (50 x 50 cm for each chamber). Spontaneous locomotion was quantified as distanced traveled at baseline (no drug) and 45 minutes following drug administration. Asymmetry of locomotion was calculated as a percentage of lesion ipsilateral to contralateral turning bias.

Abnormal involuntary movements

Abnormal involuntary movements (AIMs) were scored using the established behavioral rating scales [10-12]. Briefly, there are four types of AIMs: 1) abnormal rotational locomotion, 2) axial AIMs, showing dystonic posturing, and severe twisting of the head or neck, 3) limb movements, with rapid, jerky movements of the front or hind limbs, and 4) orofacial movements of abnormal chewing, licking, grooming, or sticking out of the tongue. The four types of AIMs were scored on a severity scale of 0-4, with 0 exhibiting no abnormality and 4 showing uninterruptable abnormal movement. AIM scores were assessed by an observer blinded to the treatment, 35 minutes post treatment injection and 20 min post L-

Dopa injection. Animals were single caged during AIM assessments. “Total AIM” scores for each animal were recorded every 20 minutes, for 1 min each, over 2 hours.

AK$^{-/-}$ forelimb and 3-paw dyskinesia

Animals were recorded in a clear plastic cylinder (16 cm in diameter and 25 cm in height) 30 minutes following L-Dopa injection. Mirrors were placed behind the cylinder to allow for ventral views of the behavior. Each trial was five minutes with a 30-second habituation period followed by behavioral scoring. The duration of abnormal paw movement was quantified for each trial and included sliding and shaking of the forelimb paws on the cylinder, and “three-paw” dyskinesia (two forelimbs and one hindlimb) and “four-paw” dyskinesia (animal balances on its tail while rearing at the glass wall) was observed in extreme cases as described in [1].

Primate MPTP model

Model preparation

The 1-methyl-4-phenyl-1,2,3,6-tetrahydropyridine (MPTP) intoxication protocol , chronic L-Dopa treatment and the clinical assessments was conducted in four male macaques (Macaca fascicularis, Xierxin, Beijing, PR of China), as previously published [13, 14]. The macaques were first rendered parkinsonian with MPTP-hydrochloride (0.2mg/kg, i.v., Sigma) dissolved in saline. Then daily (at 9 am) assessment of parkinsonism in home cages for 30 min by two blinded observers was done using a validated rating scale assessing tremor, general level of activity, body posture (flexion of spine), vocalization, freezing and frequency of arm movements and rigidity (for each upper limb). Once parkinsonism was stable, levodopa (Madopar®, Roche, Levodopa/carbidopa, ratio 4:1) was administered twice daily for 4-5 months at an individually-tailored dose designed to produce a full reversal of the parkinsonian condition (p.o. by gavage). Over this period, animals developed severe and reproducible dyskinesia, presenting choreic–athetoid (characterized by constant writhing and jerking motions), dystonic and sometimes ballistic movements (large-amplitude flinging, flailing movements), as seen in long-term L-Dopa-treated PD patients. SAG (3, 9, 27mg/kg) was dissolved in 10% DMSO, 45% HPCD in 0.9% saline and administered i.v.. Within subject escalation was performed with washout period of three days.

Immediately after drug administration, we transferred the monkeys to an observation cage (dimensions - 1.1m x 1.5m x 1.1m) as per guidelines [15]. The total duration of observation was 240 min post-gas exposure. We performed a battery of behavioural observations as previously described [13]. Experts blinded to the treatment observed 10-min video recordings taken every 30 min throughout the duration of the experiment and scored the severity of the parkinsonian condition using the parkinsonian disability score. The parkinsonian disability score is a combination of four different scores: (i) the range of movement score, (ii) bradykinesia score, (iii) posture score, and (iv) tremor score. These four scores are combined using formula: (4 - range of movement) + bradykinesia + postural abnormality + tremor. We rated the severity of dyskinesia using the Dyskinesia Disability Scale [15]: 0, dyskinesia absent; 1, mild, fleeting, and rare dyskinetic postures and movements; 2, moderate, more prominent abnormal movements, but not interfering significantly with normal behaviour; 3, marked, frequent and, at times, continuous dyskinesia intruding on the normal repertoire of activity; or, 4, severe, virtually continuous dyskinetic activity replacing normal behaviour and disabling to the animal.

We presented the time course of parkinsonian disability and dyskinesia scores in 30 min time bins over the 4 hours observation period. We also presented the median of the total scores of disability,

dyskinesia, chorea and dystonia at 0-2 hours following treatment. We statistically compared the parkinsonian and dyskinesia scores between different conditions using a Friedman's test followed by Dunn's multiple comparison test.

Optogenetic manipulations

Implant construction and implantation

Implants and patch cables were constructed and polished as previously described [16]. Mice were anesthetized with isoflourene and the surgical field was prepared with betadine. Bupivacaine was injected in the scalp prior to incision. Bregma was visualized with 3% hydrogen peroxide and a craniotomy was made over the injection site. The AAV5-EF1a-DIO-hChR2(H134R)-eYFP-WPRE virus (UNC Vector Core) was injected at AP -3.2 mm, ML +1.5 mm, DV -4.3 mm by pressure injection with a pulled glass pipette and allowed to dwell for 10 minutes. A ferrule implant was placed at AP -3.2 mm, ML +1.5 mm, DV -4.2 mm, secured with metabond, and protected with a dust cap (Thor Labs). Following surgery, mice were given 0.05 mg/kg buprenex and recovered on a heating pad. At least one month was allowed for viral expression.

Optogenetic stimulation paradigms

One trial of stimulation consisted of a ten-minute habituation period followed by an hour of intermittent stimulation of 5 sec of 10 msec long pulses at 60 Hz with a laser power of 20 mW measured at the tip of the implant, followed by a 30 sec pause. Stimulation was controlled via a TTL pulse from Ethovision's software to a Doric four channel pulse generator controlling a 710 nm Laserglow DPPS laser. All sessions were recorded and analyzed with Ethovision. Pharmacological agents were given 30 minutes prior to the beginning of the trial.

Optogenetic-induced dyskinesia

For optogenetic-induced dyskinesia (OID) experiments, stimulation occurred in a 5L glass cylinder and consisted of one hour of intermittent stimulation as previously described. Stimulation occurred daily for the duration of the experiments. A second camera (Casio EX-FH100) recorded behavior from the side of the cylinder during the first and last ten minutes of the trial. AIMs were assessed on limb, orofacial, and axial movements using the same scoring scale developed for the unilateral 6-OHDA lesion paradigm [11]. AIMs were scored separately during stimulation and non-stimulation periods. Pharmacological agents were given 15 minutes prior to the beginning of the trial.

Immunohistochemistry

Animals were anesthetized with pentobarbital (10 mg/ml) 30 minutes after last drug injection and transcardially perfused with 50 ml of 4% paraformaldehyde (PFA) in 0.2M Phosphate buffer PH 7.2. The brains were extracted and fixed overnight in 4% PFA and equilibrated in 30% sterile sucrose for 48 h. Brains were mounted in OTC and cryo-sections produced at 40 μm. Slices were incubated with antibodies as described in [17]. Sections were mounted in Vectashield (Vector Laboratories Inc.).

Confocal microscopy was performed using a Zeiss LMS 810 laser-scanning confocal microscope using the same acquisition parameters for experimental and control tissue for each experiment. Regions of interest (ROI) in the dorsolateral and dorsomedial striatum were defined guided by the pattern of the density of Shh carrying neuropil (myristylated GFP, extended data Fig. 7).

TH immunofluorescence intensity was quantified in the striatum with MacBiophotonics Image J, and the data represented mean gray levels above background.

The fraction of $pErk^{1/2}$ positive CINs was expressed as a percentage of $pErk^{1/2}$ positive CIN out of the total number of CIN in each of 375 x 375 µm ROIs in the dorsolateral and dorsomedial striatum of each coronal section analyzed. Relative position of the ROI box was kept the same between genotypes and treatment groups and along the anterior posterior axis. Quantification was performed blinded to the treatment and/or genotype of the subject in three striatal slices: anterior (AP: ~1.34 mm), middle (AP: ~0.74 mm), and posterior (AP: ~0.14 mm) per animal. Co-stained and single stained cells were manually counted using FIJI/ImageJ software (NIH). Each data point reflects the fraction of $pErk^{1/2}$ positive CIN in one ROI.

Quantification of myrGFP stained neuropil in the striatum

myrGFP stained neuropil analysis was done by transforming complete striatal sections into heat maps using Image J. Pixel intensity was quantified in the dorsolateral and dorsomedial striatum (extended data Fig. 7).

p-rpS6$^{240/244}$ Analysis

The mean grey value of p-rpS6$^{240/244}$ intensity was measured in FIJI/ImageJ software (NIH) using a freehand ROI area delineating the soma of each ChAT stained CIN in a 375 x 375 mm box in the dorso lateral striatum (extended data Fig. 9 and as described in [18]. NeuN fluorescence intensity of the same cell was used for normalization of fluorescence across treatment and genotype groups. Heat map images reveal the intensity levels of p-rpS6$^{240/244}$ fluorescence based on a 16 pseudocolor palette. 200-300 CINs were quantified per each condition.

Statistics

No statistical methods were used to predetermine sample size.

Multiple comparisons were analyzed using 2-way, 3-way, or repeated measures (RM) ANOVA with GraphPad Prism 8.0 software, followed by post hoc Bonferroni's test for specific comparisons. For 2-group comparisons, 2-tailed paired or unpaired Student's *t* test was used. Nonparametric statistics were used to verify all main effects using Dunnett's multiple comparison test or Mann-Whitney test when appropriate.

1. Ding, Y., et al., *Chronic 3,4-Dihydroxyphenylalanine Treatment Induces Dyskinesia in Aphakia Mice, a Novel Genetic Model of Parkinson's Disease.* Neurobiology of disease, 2007. **27**(1): p. 11-23.
2. Hwang, D.-Y., et al., *Selective loss of dopaminergic neurons in the substantia nigra of Pitx3-deficient aphakia mice.* Molecular Brain Research, 2003. **114**(2): p. 123-131.
3. Gonzalez-Reyes, L.E., et al., *Sonic Hedgehog Maintains Cellular and Neurochemical Homeostasis in the Adult Nigrostriatal Circuit.* Neuron, 2012. **75**(2): p. 306-319.
4. Machold, R., et al., *Sonic hedgehog is required for progenitor cell maintenance in telencephalic stem cell niches.* Neuron, 2003. **39**(6): p. 937-50.
5. Rossi, J., et al., *Melanocortin-4 Receptors Expressed by Cholinergic Neurons Regulate Energy Balance and Glucose Homeostasis.* Cell Metabolism, 2011. **13**(2): p. 195-204.
6. Jeong, J., et al., *Hedgehog signaling in the neural crest cells regulates the patterning and growth of facial primordia.* Genes & development, 2004. **18**(8): p. 937-51.
7. Harfe, B.D., et al., *Evidence for an Expansion-Based Temporal Shh Gradient in Specifying Vertebrate Digit Identities.* Cell, 2004. **118**(4): p. 517-528.
8. Muzumdar, M.D., et al., *A global double-fluorescent Cre reporter mouse.* genesis, 2007. **45**(9): p. 593-605.
9. Francardo, V., et al., *Impact of the lesion procedure on the profiles of motor impairment and molecular responsiveness to L-DOPA in the 6-hydroxydopamine mouse model of Parkinson's disease.* Neurobiology of Disease, 2011. **42**(3): p. 327-340.
10. Lundblad, M., et al., *Pharmacological validation of behavioural measures of akinesia and dyskinesia in a rat model of Parkinson's disease.* European Journal of Neuroscience, 2002. **15**(1): p. 120-132.
11. Cenci, M.A. and M. Lundblad, *Ratings of L-DOPA-Induced Dyskinesia in the Unilateral 6-OHDA Lesion Model of Parkinson's Disease in Rats and Mice.* Current Protocols in Neuroscience, 2007. **41**(1): p. 9.25.1-9.25.23.
12. Sebastianutto, I., et al., *Validation of an improved scale for rating l-DOPA-induced dyskinesia in the mouse and effects of specific dopamine receptor antagonists.* Neurobiology of disease, 2016. **96**: p. 156-170.
13. Aubert, I., et al., *Increased D1 dopamine receptor signaling in levodopa-induced dyskinesia.* Ann Neurol, 2005. **57**(1): p. 17-26.
14. Berton, O., et al., *Striatal overexpression of DeltaJunD resets L-DOPA-induced dyskinesia in a primate model of Parkinson disease.* Biol Psychiatry, 2009. **66**(6): p. 554-61.
15. Fox, S.H., et al., *A critique of available scales and presentation of the Non-Human Primate Dyskinesia Rating Scale.* Mov Disord, 2012. **27**(11): p. 1373-8.
16. Sparta, D.R., et al., *Construction of implantable optical fibers for long-term optogenetic manipulation of neural circuits.* Nature Protocols, 2012. **7**(1): p. 12-23.
17. Alcacer, C., et al., *Gαolf Mutation Allows Parsing the Role of cAMP-Dependent and Extracellular Signal-Regulated Kinase-Dependent Signaling in L-3,4-Dihydroxyphenylalanine-Induced Dyskinesia.* The Journal of Neuroscience, 2012. **32**(17): p. 5900-5910.
18. Bertran-Gonzalez, J., et al., *Striatal Cholinergic Interneurons Display Activity-Related Phosphorylation of Ribosomal Protein S6.* PLOS ONE, 2012. **7**(12): p. e53195.